Title: The bending strength of tablets with a breaking line — Comparison of the results of an elastic and a “brittle cracking” finite element model with experimental findings.

Author: Fridrun Podczeck J. Michael Newton Paul Fromme

PII: S0378-5173(15)30201-5
DOI: http://dx.doi.org/doi:10.1016/j.ijpharm.2015.09.004
Reference: IJP 15189

To appear in: *International Journal of Pharmaceutics*

Received date: 13-7-2015
Revised date: 1-9-2015
Accepted date: 5-9-2015

Please cite this article as: Podczeck, Fridrun, Newton, J.Michael, Fromme, Paul, The bending strength of tablets with a breaking line mdash Comparison of the results of an elastic and a “brittle cracking” finite element model with experimental findings.International Journal of Pharmaceutics http://dx.doi.org/10.1016/j.ijpharm.2015.09.004

The bending strength of tablets with a breaking line – Comparison of the results of an elastic and a "brittle cracking" finite element model with experimental findings.

Fridrun Podczeck*, J. Michael Newton, Paul Fromme

University College London, Department of Mechanical Engineering, Torrington Place, London WC1E 7JE, UK.

*Corresponding author. Tel. +44 20 7679 7178; fax: +44 20 7388 0180. *E-mail address*: f.podczeck@ucl.ac.uk (F. Podczeck).

Graphical Abstract

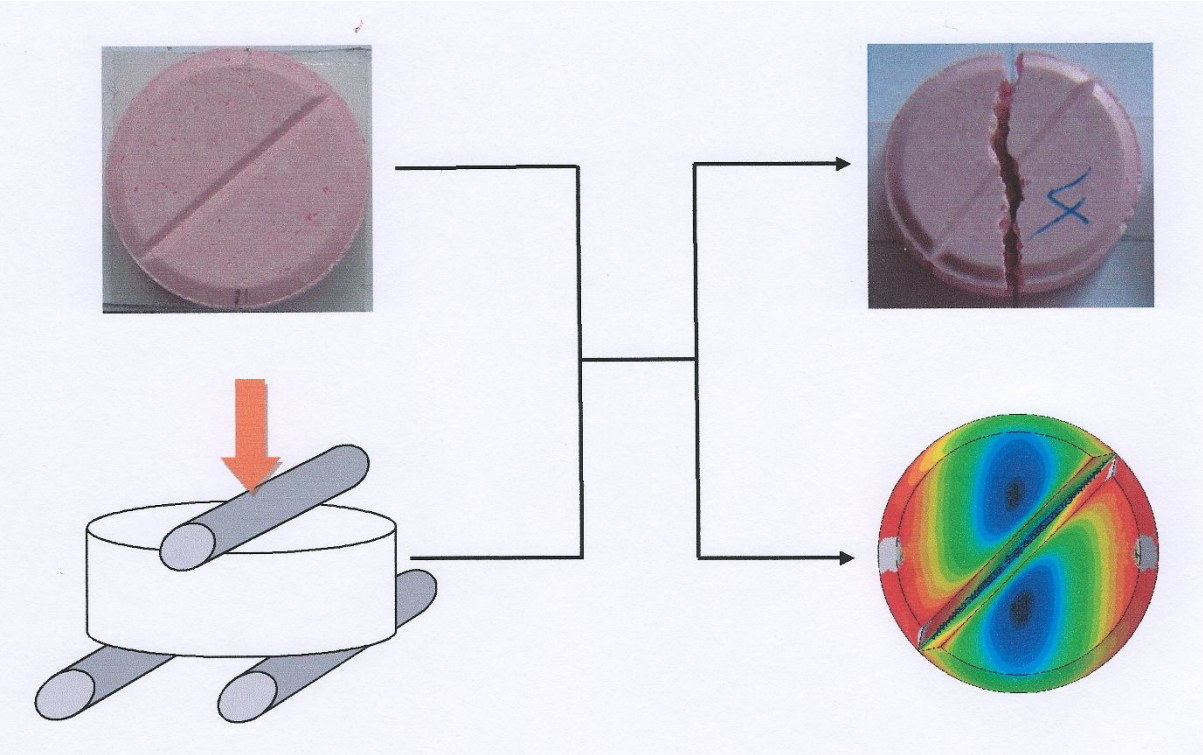

ABSTRACT

The aim of this work was to ascertain the influence of the position of the breaking line of bevel-edged tablets in a three-point bending test. Two different brands of commercially available, flat-round, bevel-edged tablets with a single central breaking line were studied. Breaking line positions tested, relative to the upper loading roll, were 0°, 22.5°, 45°, 67.5° and 90°. The breaking line faced either up- or downwards during the test. The practical results were compared with FEM results simulating similar test configurations.

Tablets failed mainly across the failure plane, resulting in two tablet halves. An exception to this was found for tablets where the breaking line faced down and was positioned at an angle of 22.5° relative to the loading plane. Here the crack followed the breaking line in the centre of the tablets and only diverged towards the loading plane position at the edges of the tablets. The breaking line facing upwards resulted in a significantly higher tensile strength of the tablets compared to it facing downwards. However, with one exception, the orientation of the breaking line relative to the loading plane appeared not to affect the tensile strength values.

A fully elastic FEM model indicated that both the position of the breaking line relative to the loading plane and as to whether the breaking line faced up- or downwards during the bending test would result in considerably different failure loads during practical experiments. The results also suggested that regardless of the breaking line position, when it is facing down crack propagation should start at the outer edges propagating towards the midpoint of the discs until failure occurs. Failure should hence always result in equal tablet halves, whereby the failure plane should coincide with the loading plane. Neither predictions fully reflected the practical behaviour of the tablets.

Using a brittle cracking FEM model significantly larger tensile stresses for tablets with the breaking line positioned downwards at 0° or 22.5° relative to the loading plane were still predicted, but the differences between model and experimental values was greatly reduced. The remaining differences are more likely due to the inadequacy of the equation available to calculate the experimental tensile strength values. This equation cannot account for the presence of a breaking line and overestimates the thickness of the loading plane by the depth of the breaking line when in 0° or 22.5° position. If the depth of the breaking line is taken into account,

the model predictions and the experimental findings are comparable. Also, in the brittle cracking FEM simulations the predicted crack propagation patterns were similar to those found in the experiments, and the model stress distributions across the lower surfaces were much more homogeneous and streamlined parallel to the loading plane. The brittle cracking model hence reflected the practicalities of the bending test more closely. The findings suggested that with the breaking line facing down fracture should always start in the centre of a tablet at its lower surface, initiated by the breaking line. Due to simultaneous development of larger stresses along the y-axis the tablet should still break into two equal halves along the loading plane, unless the position of the breaking line relative to the loading plane was 22.5°. In this case the tablet would fail by a mixed process, whereby failure would occur mainly along the breaking line, but due to simultaneous crack formation at the lower surface close to the bevel edge parallel to the loading plane the final breaking pattern would deviate from the breaking line about half-way from its centre, as seen in the practical experiments.

Keywords:

Bevel-edge

Breaking line

Brittle cracking

Finite element method (FEM)

Tablet tensile strength

Three-point bending

1. Introduction

In an attempt to reduce chipping of the tablet edges during packaging, transport and handling, flat round tablets typically are bevel-edged. Frequently they also have a breaking line ("score line"), the purpose of which has been discussed by Van Santen et al. (2002). Under industrial manufacturing conditions, the breaking force of round tablets should be tested using the standard diametral compression test (Method 1217, USP38/NF33, 2014). Recently, Podczeck et al. (2014) investigated the influence of the position of the breaking line in terms of its angle relative to the loading plane during a diametral compression test of commercially available bevel-edged flat-round tablets. They compared their practical findings with theoretical investigations using finite element method (FEM). FEM results using both a fully elastic and an elasto-plastic model predicted that the tensile stress values at failure would be up to three times larger, if the breaking line was positioned at an angle of less than 45° relative to the loading plane, whereas at an angle of 45° or larger the failure loads should be similar. Newton et al. (1977) using photoelasticity measurements reported that the effect of the breaking line position depended on its depth, and if the depth was in the range of commercial tablet designs, a horizontal breaking line position caused compressive stresses at the tip of the breaking line and was associated with an increase in tensile stresses at the plane face. On the other hand, the vertical position of the breaking line resulted in increased tensile stresses at the tip of the breaking line and a reduction in the tensile stresses at the flat face. Similar effects, but more detailed due to the use of different breaking line positions in terms of angles relative to the loading plane, were found using FEM (Podczeck et al., 2014), and their theoretic work also predicted that not all breaking line angles would result in clean tensile failure. The practical results, however, only confirmed some deviations from a clean tensile failure due to the position of the breaking line, whereas the breaking forces as such were only marginally affected by the position of the breaking line relative to the loading plane. Since there were differences in the breaking pattern, they concluded that despite similar failure loads the failure mechanism varied with the angle of the breaking line and hence a conversion of a breaking load into the tensile strength using the Brazilian equation (Barcellos, 1953; Carneiro, 1953; Fell and Newton, 1968, 1970) was not recommended.

Mazel et al. (2014) suggested that pharmaceutical compacts of round, cylindrical shape should be tested using a three-point bending test, because it reflects the tensile failure stress more accurately than the diametral compression test. The advantages and disadvantages of this test in terms of its practical applicability under routine settings in the pharmaceutical industry can be found in previous reports (Podczeck, 2012; Podczeck et al., 2014). However, this test has not yet been studied in terms of its applicability and accuracy when breaking round-flat, bevel-edged tablets with a breaking line.

The aim of this work was to ascertain the influence of the position of the breaking line in a three-point bending test. Similarly to the previous paper (Podczeck et al., 2014) two different brands of commercially available, flat-round, bevel-edged tablets with a single central breaking line were studied. Breaking line positions tested, relative to the upper loading roll, were 0°, 22.5°, 45°, 67.5° and 90°. The breaking line was either facing down or upwards during the test. The down-facing position would be theoretically preferred due to tensile stresses developing only at the lower tablet face during a bending test and crack propagation leading to tablet failure should hence always start at the lower tablet surface. In this situation, fracture mechanics predicts a stress concentration at the tip of the breaking line (Irwin, 1957), and thus potentially an influence of the breaking line position on the failure stress. However, assuming that under industrial working conditions an automatic tablet positioning mechanism would be required to make such a test viable, an upwards orientation of the breaking line appears possible and hence should also be investigated. The practical results were then compared with FEM results simulating similar test configurations. Initially an elastic model was employed, followed by a brittle cracking model in an attempt to overcome discrepancies between the theoretical FEM results and the experimental findings.

2. Materials and Methods

2.1. Software

Standard finite element methodology (FEM) was employed (Abaqus 6.12.3, Dassault Systèmes, Vélizy-Villacoublay, France). Cubic-spline interpolations were made using a Microsoft®-approved add-on to Excel 2013 (SRS1 Software, Boston, MA). Analysis of Variance (ANOVA) was performed using SPSS 20.0 (SPSS-IBM, Woking, UK).

2.2. Practical work

Bevel-edged tablets with a single central breaking line were purchased to be able to reflect the larger variability of tablet breaking loads of commercially produced compacts during testing: (1) Superdrug Diarrhoea Relief Tablets (DRT), Surepharm Services Ltd., Burton-Upon-Trent, UK, batch 4A222; (2) Boots Aspirin 300 mg Dispersible Tablets (ADT), Aspar Pharmaceuticals Ltd., London, UK, batch 140700.

According to the Patient Information Leaflet (PIL) the main ingredients of the DRT tablets are 400 mg light kaolin and 75 mg calcium carbonate. The remaining excipients are icing sugar, maize starch, magnesium stearate, erythrosine, clove-, cinnamon- and nutmeg oil. The estimated powder particle density of the mixture is 2150 kg m^{-3}. The ADT tablets contain 300 mg of acetylsalicylic acid, plus lactose monohydrate, sodium saccharin, maize starch, citric acid, sodium lauryl sulphate, talc and calcium carbonate as excipients (based on updated “Summary of Product Characteristics”, dated 27 April 2015). The estimated powder particle density of the mixture is 1470 kg m^{-3}.

The breaking load of the tablets was determined using a CT6 tablet strength tester (Engineering Systems, Nottingham, UK), equipped with a 50 kg load cell, at a test speed of 1 mm min^{-1}. A three-point bending rig was used, which had freely rotating lower rolls and a fixed upper roll, each of 3 mm diameter. The distance between the midpoints of the lower rolls was 10.5 mm. The breaking load was recorded with an accuracy of ±0.005 kg. The tester was linked to a laptop (Dell Latitude D505, Dell UK, Bracknell, Berkshire) via a USB cable. Machine inherent plotter software (Graph Plotter®, V2.09; Engineering Systems, Nottingham, UK) was installed and used to control the tester remotely from the computer. Force versus displacement curves were recorded for each tablet using a recording frequency of 1000 Hz. They were

exported into Windows Excel 2007 (Microsoft®) and further processed to obtain the slope of the linear portion of the force-displacement curves. The tensile failure stress of the tablets was calculated from (Hertzberg, 1996):

$$\sigma_t = \frac{3PL}{2DW^2} \qquad (1)$$

where *P* is the breaking load, *L* is the distance between the midpoints of the lower rolls, and *D* and *W* are the diameter and thickness of the tablet, respectively.

Tablets were weighed to ±0.001 g (Sartorius BP 121S, Göttingen, Germany) and their dimensions were measured to ±0.001 mm (Moore and Wright MED961D Digital Micrometer, Neill Tools Ltd., Sheffield, UK). A protractor was used to mark the exact test positions for the tablets to be placed between the loading platens of the CT6.

To determine the exact cup depth and width of the breaking line, photographs (Olympus SP-500UZ, Olympus Imaging Corp., Hamburg, Germany) of the tablets were taken with a magnification of x50 (diameter view) and x100 (thickness view) against a graticule (Graticule Ltd., Tonbridge, UK).

2.3. FEM model description

The basic terminology used for flat, round, bevel-edged tablets with a breaking line is shown in Fig. 1a. A 3D FEM model was employed to study tablets subjected to three-point bending. The tablet dimensions were chosen to match those of the commercially produced, practically tested tablets i.e. a thickness (*W*) to diameter (*D*) ratio of 0.286, a bevel angle of α = 30°, a cup depth of 14.4% of the total tablet thickness and a single breaking line with an opening angle of 90° and a depth matching the bevel were investigated in the models. Comparisons were made between (a) fully flat and bevel-edged tablets, and (b) between bevel-edged tablets having a breaking line at different positions φ during loading i.e. breaking line positions tested were 0°, 22.5°, 45°, 67.5° and 90° (Fig 1b). Breaking lines were positioned to face either downwards or upwards.

Since the position of the breaking line results in unsymmetrical test configurations, complete tablets were modelled. The bender design matched that of the CT6 used in the practical experiments, having a roll diameter of 3 mm and a distance between the

centre points of the lower rolls of 10.5 mm. However, only the halves of the rolls in contact with the tablet were simulated (Fig. 1b). Boundary conditions (Fig. 1b) were applied to the rolls to avoid tilting, slipping, sliding or twisting and only to permit movements parallel with the loading plane. Directional boundary conditions are signified with *u* and rotational boundary conditions are signified with *R*. To hold the tablets in place and to avoid large localised penetrations of the tablets, a surface-to-surface discretization approach was used and a friction coefficient between the upper loading roll and the tablet surface of μ=0.1 was assumed. Surface smoothing was applied to the roll and tablet surfaces to avoid the need of matching nodes across the contact interface and an iterative solver algorithm was chosen. 3D-quadratic tetrahedral elements (C3D10) were used for the meshing. The mesh density to achieve a stable and accurate solution was optimised using a convergence test as described earlier (Podczeck et al., 2013). The mesh density of the rolls (s=0.001) was kept slightly below that of the tablets (s=0.0008) to ensure convergence.

A reverse rainbow colour scheme was employed to visualise the stress distributions of the deformed discs. All compressive stresses were coloured in grey. The total spectrum was split into 16 different colour grades between red (lowest tensile stresses) to dark blue (highest tensile stresses).

The stainless steel rolls were modelled from engineering steel with a Young's modulus of 209 GPa and a Poisson's ratio of 0.3. The load *P* was transmitted by ramp loading through the top roll, and assuming fully elastic behaviour, for a flat disc this would result in a maximum tensile stress of 1.32 MPa. The load was kept constant for all models. Similar to previous work (Podczeck et al., 2013, 2014) only one linear elastic model with the properties of Araldite CT200, hardened with 30% w/w Hardener 901, for which Young's modulus of elasticity (2.58 GPa) and Poisson's ratio (0.35) were taken from the literature (Burger, 1969), was studied. The theory of elasticity (Timoshenko and Goodier, 1987) predicts that relative stress distributions are independent of Young's modulus and Poisson's ratio, and that this holds in FEM studies has previously been confirmed (Pitt and Heasley, 2013, Podczeck et al., 2013). There is therefore no need to repeat the analyses with other elasticity data.

A brittle-cracking model was also employed. This is normally used to model concrete, ceramics, brittle rocks and other materials behaving in a similar fashion. The similarity between ceramics and powder compacts is well known (Stanley and

Newton, 1978) and has been exploited in pharmaceutical research many times (e.g., Duncan-Hewitt and Weatherly, 1989; Mashadi and Newton, 1987, 1988; Roberts and Rowe, 1987; Roberts et al., 1993; Podczeck, 2001a,b, 2002, 2011). The behaviour of the structures has to be dominated by tensile cracking and it is assumed that the compressive behaviour of the structures is linear-elastic. These criteria are fulfilled in the three-point bending test of a tablet (Stanley, 2001). In Abaqus, the model is an extension of the linear elastic material model. Although there are various options, in this paper crack detection was based on mode I fracture mechanics principles (i.e. opening or tensile mode with the crack surfaces moving directly apart). The basics of mode I failure is described by Hertzberg (1996). For the FEM brittle-cracking model used in this work, the powder material properties of relevance are listed in Table 1. The choice is based on the composition of the Boots Aspirin Dispersible Tablets, because their main ingredients are acetylsalicylic acid and lactose monohydrate. For light kaolin, which forms the bulk of the Superdrug Diarrhoea Relief Tablets, fracture mechanics data are not available. The shear retention factor and the direct cracking failure strain were obtained from the force-displacement curves recorded during the practical experiments (section 2.2.) and kept constant during all simulations.

The brittle cracking FEM model has to be run as an Explicit-dynamic model, which differs from a static model such as the fully elastic model not only in the material properties (described above), but also in the contact model, the elements and the loading properties. The elements are still 3D-quadratic tetrahedral (C3D10M), but the Explicit-dynamic model uses a general contact model with overall contact friction. The load was applied as a step-load, and the response of the model was monitored. All other model parameters are as for the fully elastic FEM model.

2.4. Statistical analysis

Analysis of Variance (ANOVA) was performed to compare the experimental findings. The post-hoc Scheffé test (Scheffé, 1959; Berry and Lindgren, 1996) was used for multiple comparisons to identify significantly different samples and sample groups. The level of significance (α-error) was set to $p=0.05$ in all cases.

3. Results and discussion

3.1. Experimental assessment of the failure properties of tablets

Table 2 summarises the properties obtained using the commercially produced tablets. Comparing Superdrug Diarrhoea Relief Tablets (DRT) and Boots Aspirin 300 mg Dispersible Tablets (ADT) tablets first separately, ANOVA confirmed that there was no significant difference between individual subgroups, i.e. different breaking line positions and the breaking line facing either up- or downwards during the test. The width of DRT and ADT tablets is statistically similar with overall average values ($n = 100$) of 3.672 ± 0.031 and 3.632 ± 0.037 mm, respectively. The tablet diameters (12.824 ± 0.010 mm and 12.987 ± 0.022 mm for DRT and ADT, respectively) are statistically significantly different ($p < 0.001$), but both close to 13 mm and therefore similar bender settings using a distance between the midpoints of the lower rolls of 10.5 mm were employed. As expected from the tablet compositions, the overall tablet weight of the ADT tablets (600 ± 8 mg) was approximately ¾ of the weight of the DRT tablets (803 ± 10) despite statistically similar tablet volumes (0.481 ± 0.005 cm^3 and 0.474 ± 0.004 cm^3 for ADT and DRT tablets, respectively).

Under industrial routine working conditions the use of a three-point bending test for tablet tensile strength measurements would require an automatic feeding and positioning system, which is currently not available. However, it appears feasible to develop such a system, but most likely it would not distinguish between the tablet face carrying the breaking line and the opposite face. Hence, in this work the breaking line was not only positioned facing downwards, which would be the orientation in line with fracture mechanics principles (Brown and Srawley, 1967; Dunn et al., 1997; Griffith, 1920; Irwin 1957; Mullier et al., 1991), but also facing upwards. The tablet tensile strength was calculated without considering the breaking line or its position, as there is no analytical solution available for this kind of specimen shape. The results are listed in Table 2. The force-displacement curves were all linear over more than 90% of their total length and similar in slope, as previously observed during diametral compression tests (Podczeck et al., 2014). This indicates that in all cases the tablets failed by unstable crack propagation due to sufficient energy being released to propagate the most suitably oriented flaw at the lower surface of the tablets. Failure occurred suddenly and completely, mainly across

the failure plane, resulting in two tablet halves. Both is typical for elastic behaviour of brittle specimen (Adams, 1985).

Although there is no steady trend describing the relationship between the position of the breaking line relative to the loading plane (Table 2) and the tensile strength of the tablets, it can be observed that the tensile strength for tablets with the breaking line at 0° is always a fraction smaller than the other values. The largest tensile strength is always seen for a breaking line position of 90°. To find out whether this tendency was statistically significant, ANOVA was used to compare the tensile strength values.

The overall tensile strength of DRT tablets with the breaking line facing upwards (1.93±0.08 MPa) is significantly higher ($p = 0.028$) than that of DRT tablets with the breaking line facing down (1.82±0.05 MPa). This demonstrates that the breaking line when facing down can lead to stress concentration at its tip. The bending stress concentrates at the tip of the breaking line, leading to tablet failure at slightly lower tensile stresses. However, for ADT tablets no statistically significant difference between tensile strength values can be detected ($p = 0.406$) when comparing the overall values of tablets with the breaking line facing either upwards (2.77±0.13 MPa) or downwards (2.71±0.10 MPa). The effect seen might hence be material dependent.

When comparing the different orientations of the breaking line using ANOVA, however, only for DRT tablets with the breaking line facing upwards a statistically significant difference in the tensile strength values can be identified ($p = 0.019$). The Scheffé-test (a multiple pair comparison technique; Berry and Lindgren, 1996) indicates that this is due to significantly smaller tensile strength values when the angle of the breaking line is 0°. In this test situation the upper loading roll (3 mm in diameter) will not only be completely aligned with the breaking line, but will penetrate the line cavity (≈1 mm opening at its top and ≈0.5 mm depth) by approximately 100 µm i.e. 20% of its depth, which prevents bending and might cause load spreading resulting in a slightly smaller value of the tensile strength.

As mentioned before, failure occurred suddenly and completely, mainly across the failure plane, resulting in two tablet halves. The exception to this was consistently found for tablets where the breaking line faced downwards and was positioned at an angle of 22.5° relative to the loading plane. As can be seen from Fig. 2a,b in this case in the centre of the tablets the crack follows the breaking line and only diverges

towards the loading plane position at the edges of the tablets. This is more pronounced for ADT tablets (Fig. 2b), but still clearly visible on DRT tablets (Fig. 2a). Examples for failure fully aligned with the loading plane are shown for ADT tablets at a 90° (Fig. 2c) and for ADT tablets at a 45° angle (Fig. 2d) of the breaking line relative to the loading plane.

3.2. FEM analysis of elastic discs

3.2.1. Evaluation of the x-axial stress distributions

The x-axial stress distribution in flat and bevel-edged elastic discs during three-point bending is compared in Fig. 3a,b. In the XZ-plane (Fig. 3a) the differences in the centre of the tablets are overall small but it can be seen that the addition of the bevel edge leads to a slightly larger tensile stress at the lower tablet face, with a ratio of the maximum tensile stress values at $x=y=0$ and $z=-0.5$ of 1.02. Due to the position of the bevel edge there is also a difference in the compressive stresses above the lower supports. This can be observed even more clearly when the x-axial stress distributions at the lower surface are compared (Fig. 3b). Due to the smaller contact area with the lower supports when bending the bevel-edged disc the tensile stresses are not as widely spread as for the flat disc. However, the oval shape of the area encompassing the central maximum tensile stresses is fairly similar (dark blue colour), which is the important aspect for failure to occur in a bending experiment.

The influence of an addition of a breaking line to the bevel-edged disc on the tensile stresses in the XZ-plane is explored in Fig. 3a. When the breaking line faces down and is parallel to the loading plane or in a position of 22.5° relative to the loading plane, a stress concentration above the tip of the breaking line can be observed (dark blue area), and at the same time the stresses at the edges of the breaking line are reduced (green to yellow colour). This effect is hardly visible for a 45° position and can no longer be seen if the breaking line position relative to the loading plane is above 45°. The stress profile at 90° is similar in appearance to that of the bevel-edged disc without breaking line. When the breaking line faces up and is positioned parallel to the loading plane, the disc cannot bend due to the loading roll penetrating the breaking line, as explained under section *3.1*. In general a more flattened x-axial stress distribution is found when the breaking line is facing upwards. Interestingly, for

a 90° position of the breaking line relative to the loading plane bending is again inhibited, but not fully suppressed. This might be due to the breaking line not being able to “fold” without opening up at the same time.

The x-axial tensile stress distribution at the lower surface of discs with the breaking line positioned at various angles relative to the loading plane and with the breaking line facing either down or up during three-point bending is explored in Fig. 3b. When the breaking line faces upwards, the stress profiles within the centre of the lower surface are similar to the bevel-edged disc. However, the narrow, symmetrical protrusions of tensile stresses near the lower supports are least pronounced for a 0° degree position of the breaking line, but they become more and more obvious the more the breaking line is twisted relative to the loading plane. It is important to note that during the experiments no failure occurred at these points, as would be expected from a correct construction and set-up of the loading rig (Stanley, 2001). The 90° position stress distribution is similar to that of the simple bevel-edged disc. When the breaking line faces down, there is a clear concentration of tensile stresses along the centre of the breaking line as long as the angle relative to the loading plane does not exceed 22.5°. At 45° the stress concentration is less focussed on the centre of the breaking line, but seems to spread towards the outer edges of the breaking line, and for all other breaking line positions it appears as though the stress within the breaking line merges with the oval-shaped stress profile along the y-axis i.e. there is no longer a stress concentration within the breaking line. This is in line with the observations made in the XZ-plane.

The absolute values of the maximum x-axial tensile stresses along the y-and z-axis for discs with the breaking line facing down, obtained using the fully elastic FEM model, are listed in Table 3. For the breaking line facing down up to eight times higher tensile stresses are predicted when comparing the 0° and the 90° position. This is, compared to the practical findings (Table 2) unrealistic. For the breaking line facing upwards, the maximum x-axial tensile stresses along the y-axis are 1.880, 1.712, 1.702, 1.668 and 1.785 MPa, for 0°, 22.5°, 45°, 67.5° and 90°, respectively. In order to compare the up and the down position of the breaking line in terms of their overall stress values, the 0° position has to be omitted because of the unrealistically high stress concentration, predicted for the breaking line facing down. The overall values are 1.749 MPa for the breaking line facing upwards, and 1.577 MPa when the

breaking line faces down. Hence, similar to the experimental findings, an upward position of the breaking line during the bending test results in a higher tensile strength than when the breaking line faces down.

3.2.2. Comparison using normalised stress values

In order to compare the numerical results between individual breaking line positions and with the bevel-edged disc, the x-axial stress values either along the z-, y- or x-axis need to be normalised. This could have been done by dividing all stress values at every point and for every disc with either a theoretical stress value (Pitt et al., 1989) or the maximum tensile stress value obtained either on the flat or the simple bevel-edged disc (Drake et al., 2007). However, either approach did not seem justified because within the simple bevel-edged disc the x-axial stresses progress along each axis rather than being constant. It was hence decided to normalise the stresses for each disc carrying a breaking line with the corresponding stresses of the simple bevel-edged disc, at each location using values matching exactly the same position along the z-, y- or x-axis. This normalisation technique had previously been used successfully by Podczeck et al. (2013).

In Fig. 4a,b the normalised x-axial stresses along the z-axis are compared for discs with a breaking line. When the breaking line faces down (Fig. 4a) the stress concentration at the tip of the breaking line can be clearly seen. It is largest for the 0° position of the breaking line relative to the loading plane and decreases with an increase in the angle of the position of the breaking line relative to the loading plane. However, at a position of 45° and above the differences are marginal. Up to a position of $2z/W=-0.4$ the x-axial tensile stresses along the z-axis are larger than observed on the simple bevel-edged disc. Then a sharp drop in the normalised x-axial stresses can be seen indicating that the tensile stresses are now less than those obtained on the simple bevel-edged disc and finally, when reaching the upper half of the disc, the compressive stresses of the bevel-edged discs with breaking line are only about one tenth of the simple bevel-edged disc. When the breaking line is positioned upwards (Fig. 4b) there is hardly any difference between the normalised x-axial stress values. As for the down-facing position initially the tensile stresses are larger than found on the simple bevel-edged disc, but all compressive stresses are again only about one tenth of those of the simple bevel-edged disk. As before there

is a sharp drop in normalised x-axial stress values at *2z/W=-0.4*. The breaking line hence increases the tensile stresses at the lower surface of the discs, regardless of the position relative to the loading plane and whether it is facing up or down, and as a result there are comparatively lower tensile stresses towards the centre of the discs.

Fig. 5a,b compares the normalised x-axial stresses along the y-axis. When the breaking line is facing downwards (Fig. 5a) a reduced stress across the lower face, presumably due the stress-concentration effect of the breaking line, can be noticed. A breaking line position relative to the loading plane of 67.5° or 90° appears to results in an increased normalised tensile stress at the lower face close to the bevel-edge. The normalised tensile stresses across the remainder of the y-axis towards the midpoint of the lower face of the discs appear similar to the simple bevel-edged disc. This would mean that the discs would start to fail from the outer edges and the two initial cracks forming at each edge would propagate almost instantaneously towards the midpoint of the discs along the loading plane until they merge and complete failure has occurred. For breaking line positions of 45° and 22.5° no such peak of normalised x-axial stresses can be seen close to the bevel-edge, but here the stresses increase gradually towards the midpoint of the lower tablet face, again indicating that the discs would start to fail from the outer edges and the two initial cracks forming at each edge would propagate towards the midpoint of the discs along the loading plane until they merge and complete failure has occurred, just that this process would be slightly slower. The 0° position does not allow a direct comparison of the stresses along the y-axis at the lower tablet face. If the breaking line faces upwards (Fig. 5b) for all tested breaking line positions the normalised stress values along the y-axis are fairly similar between each other and when compared to the simple bevel-edged disc. Such a more homogeneous stress development across the centre line of the lower tablet face would normally be expected; the slight curvature of the stress profiles is caused solely by the bevel-edge.

Finally, the normalised x-axial stresses along the x-axis at the lower face of the discs are compared in Fig. 6a,b. The tensile stresses of discs with the breaking line facing down are elevated close to the position of the breaking line, then drop sharply, but immediately start to rise again to reach a second maximum value between *2x/D=0.65-0.75*. Up to this point the tensile stresses are higher than those found on

the simple bevel-edged disc. The maximum values are followed by a sharp drop and irregular ups and downs of the normalised stress values, which is presumably a result of the proximity to the lower support rolls and overlapping of compressive and tensile stresses. The findings again indicate a clear influence of the breaking line on stress development and stress concentrations, which should result in clearly different tensile strength values in practice. When the breaking line faces upwards, however (Fig. 6b), an effect of the breaking line in terms of stress concentration cannot be seen except for the 90° position, but as before the x-axial tensile stresses are larger when a breaking line is present, compared to a simple bevel-edged disc. As before the variations close to the bevel-edge are due to the overlapping of compressive end tensile stresses at the lower supports. The higher tensile strength values predicted for the 90° orientation of the breaking line relative to the loading plane coincide with the lower capability of the disc to bend, as reported in Fig. 3a.

The findings presented using a fully elastic FEM model predict that both the position of the breaking line relative to the loading plane and as to whether the breaking line faces up- or downwards during the bending test should result in considerably different failure loads during experimental testing of tablets with a breaking line. However, in the practical experiments such significant differences were not observed (Table 2). The results also suggest that regardless of the breaking line position, when it is facing down crack propagation will start at the outer edges propagating towards the midpoint of the discs until failure occurs. Failure should hence always result in equal tablet halves, whereby the failure plane should coincide with the loading plane. In practice the latter was not observed when the breaking line was at a 22.5° position relative to the loading plane (see Fig. 2). Hence, the FEM results based on a fully elastic model do not fully reflect the practical behaviour of the tablets. A similar observation had been made previously when modelling the diametral compression test (Podczeck et al., 2014).

3.3. FEM analysis using a “brittle cracking” model

3.3.1. General approach

To resolve the discrepancies between the practical findings and the predictions based on a fully elastic FEM model, it was now assumed that the tablets behaved

brittle during the test, similar to concrete or ceramic specimens (Stanley and Newton, 1978; Stanley, 2001). In this case it is important to use material properties that are similar to the properties of the composite material represented by the tablets. The required fracture mechanics data are, however, sparsely reported in the literature, and they show gross discrepancies between authors (Bin Baie et al., 1996). Light kaolin, which is the major ingredient in DRT tablets, does not form firm compacts on its own, which makes it impossible to obtain reliable experimental data. On the other hand, both acetylsalicylic acid and lactose monohydrate – the two main components of the ADT tablets – have been studied in house and a full set of reliable fracture mechanics data is hence available (Podczeck, 2001a,b, 2002). In view of the composition of the ADT tablets, it is an advantage that data for a 1:1 (v/v) mixture of the two powders have also been studied (Podczeck, 2011). Hence the material properties of acetylsalicylic acid, lactose monohydrate and their 1:1 (v/v) mixture were used in the brittle cracking FEM models (Table 1). Acetylsalicylic acid has been described as a ductile material (Jetzer et al., 1984) showing plastic deformation combined with limited propensity to fragmentation up to a tabletting pressure of 45 MPa (Humbert-Droz et al., 1983). At higher compaction pressures predominantly elastic deformation behaviour has also been described (Mielck and Stark, 1995). Podczeck (2001a) reported that acetylsalicylic acid behaved ductile; at lower compaction pressures plastic flow dominated whereas at compaction pressures above 150 MPa brittleness was observed. Contradicting reports for lactose monohydrate describe it as either ductile (Duberg and Nyström, 1982; Podczeck, 2001a) or brittle (Cole et al., 1975; Mielck and Stark, 1995). Table 1 demonstrates that there are sufficient differences in material properties of the individual powders and the powder mixture, which, if important for the failure of the tablets, should result in different FEM results. In particular there is a 2.5-fold difference in the maximum failure stress of the materials and a two-fold difference in the Young's modulus of elasticity.

The fully elastic model did not reveal major differences in normalised stress values between the discs with difference breaking line positions relative to the loading plane when tested with the breaking line facing upwards. As this was in line with the practical findings, the brittle cracking model was only applied to discs where the breaking line faced down. In Fig. 4c, 5c, 6c and 7a,b the findings for lactose

monohydrate are reported as an example of the outcome using the brittle cracking model.

3.3.2. Evaluation of crack formation and x-axial stress distributions

As can be seen from Fig 7a, for a simple bevel-edged disc a sharp crack formation cannot be observed. However, a sharp crack running along the centre of the breaking line is clearly visible when the breaking line is positioned at 0° or 22.5° relative to the loading plane. At 45° a crack still appears to propagate along the breaking line, but is less sharp. When the breaking line is in a 67.5° or 90° position relative to the loading plane, the crack appears not to propagate along the breaking line. Fig. 7b demonstrates that in a simple bevel-edged disc the crack propagates along the y-axis parallel to the loading plane, starting in the centre and propagating towards the bevel edges. If the breaking line is in the 0° position relative to the loading plane, the crack propagates at the lower surface along the centre of the breaking line, from the midpoint outwards. At a 22.5° angle between the breaking line and the loading plane the crack still propagates from the midpoint of the breaking line along it, but at the same time there is some crack formation at the upper and lower end of the disc close to the bevel edge. This would indicate a mixed failure, whereby the failure would occur mainly along the breaking line, but would veer off this path due to simultaneous crack formation at the lower surface of the disc close to the bevel edge parallel to the loading plane. The findings for the 0° and 22.5° position of the breaking line relative to the loading plane are in agreement with the observations made during the experiments (Fig. 2a,b). At a position of 45 ° there is still considerable crack propagation in the centre of the disc along the breaking line, but at the same time mirror-image cracks propagate from the centre of the lower surface towards the outer bevel-edge of the disc, parallel with the loading plane. With an increase in the angle between the breaking line and the loading plane the crack propagation along the breaking line decreases, whereas domineering mirror-image cracks propagate from the centre of the lower surface towards the outer bevel-edge of the discs indicating that the discs would split in two halves following the path of the loading plane. Again this is in good agreement with the practical findings shown in Figure 2c,d. Compared to the FEM results of a fully elastic material, in the brittle cracking model the stress distributions across the lower surfaces are much more

homogeneous and streamlined parallel to the loading plane (Fig. 7b), as would be expected in a bending experiment. In this respect the brittle cracking model reflects the reality of the test better.

The differences in normalised x-axial stresses along the z-axis between the fully elastic and the brittle cracking FEM model can be seen when comparing Fig. 4a with Fig. 4c. The brittle cracking model still predicts stress concentrations at the tip of the breaking lines for a 0° and 22.5° position of the breaking line, but the degree is clearly reduced from four-fold (fully elastic model) to 2.5-fold, when the 0° position is compared. In theory this should still lead to a difference in the tensile strength of tablets with the breaking line in this position compared to those where the breaking line is in the 45° position or above relative to the loading plane, but in the practical experiments such a difference was not found (Table 2). This can also be seen from the maximum x-axial tensile stresses predicted along the y- and z-axis (Table 3), which suggest a three-fold larger tensile strength for tablets where the breaking line is positioned parallel to the loading plane (0°). The origin of this discrepancy might lie in the porosity (≈ 15%; Table 2) of the tablets compared to a non-porous disc used in the FEM simulations. Tensile stresses will be reduced due to the presence of pores for a number of reasons. For example, porosity values similar to those of the tested tablets (11-17%) reduced the load-bearing capacity of specimens during a three-point beam bending test (Fleck and Smith, 1981). Lattice effects can also reduce the practically found tensile failure stress by reducing the stress concentration ahead of the propagating crack (Rice, 1978), i.e. while it is assumed that all bonds within the compact structure behave fully linear-elastic during deformation, those bridging the crack plane might show non-linear behaviour. Pores are not only simple stress concentrators that accentuate failure due to other flaws (Rice, 1989). They often, but not always, form an integral part of the failure-causing flaws during tensile testing (Evans and Tapping, 1972; Rice, 1984), and they can also act themselves as fracture origin (Boccaccini, 1999). Wu et al. (2005) prepared rectangular powder compacts (7×7 mm) from coarse-grade sodium chloride using uniaxial compression. Their test porosity was 30% i.e. considerably larger than that of the studied DRT and ADT tablets, which most likely were also produced on a rotary die machine. Nevertheless, when neglecting the increase in porosity towards the bottom of the compact, which is purely the result of uniaxial compression (Train, 1957), the results revealed a preferential orientation of the pores in the direction of the compressive

force i.e. an orientation advantageous for crack propagation during a bending test. Charlton and Newton (1985) reported that the porosity of compacts will be reduced in the corners nearest to the moving tabletting tools. The breaking line adds an additional region of low compact porosity to the bevel-edged tablets. This will result in differences in the location of pores large enough to weaken the tablet structure and suggests that crack propagation might start at a pore above but not forming part of the breaking line. All these aspects should result in a smaller experimental failure load and hence lower tensile strength than predicted in the brittle cracking model.

Many engineers, for example Rice (1994), have questioned the validity of extrapolations to zero porosity to obtain material data such as those presented in Table 1, because there might be an abrupt change from a pore-determined to other flaw-determined failure at or close to zero porosity. Mechanical properties such as tensile strength also do not only depend on the average specimen porosity, but more specifically on the size of the pores and their orientation. Both high porosity and low porosity, when combined with a large pore size, will result in weaker mechanical strength, compared to specimen with high or low porosity and small pore size (Szibor and Hennicke, 1982). However, the use of single crystal data to obtain mechanical material properties is equally troublesome due to crystal anisotropy and hence to date the material properties of pharmaceutical powders can only be estimated with some degree of confidence using zero-porosity extrapolations. Podczeck (2001a, 2011) used very fine grades of acetylsalicylic acid and lactose monohydrate (particle size distribution well below 10 µm) when studying the fracture mechanics properties of the materials listed in Table 1. This was done in order to achieve specimen porosity values close to zero to ensure accurate extrapolations of the data to zero porosity. It is likely that the particle size distribution of the powders used to manufacture the ADT tablets, although chemically identical, was larger, which would result in different pore sizes and pore size distributions. Such particle size effects on pore size and pore size distributions were, for example, reported by Nicklasson and Podczeck (2007), who found a significant decrease in extrapolated zero-porosity values such as maximum failure stress and critical stress intensity factor with increasing pore size distribution.

In the studied tablets, pores are present and they will most likely be surrounded by a number of cracks with random orientations, but in the FEM models used it is

assumed that there is only one single crack present at the maximum stress point i.e. the breaking line. In reality the breaking line will introduce an overall (macroscopic) stress concentration, and the pores within that region will introduce an additional small-scale (microscopic) stress concentration. As a result, the “brittle cracking” FEM model, which is based on a non-porous specimen that follows the laws of linear elastic fracture mechanics, might overestimate the stress concentration at the tip of the breaking line and along the y-axis to some extent. If it is assumed that within the tested tablets the presence of a larger degree of porosity and larger pore sizes will have resulted in some stress concentration at the tip of the breaking line but at the same time also at the tip of a suitably sized and oriented crack near the maximum stress point, then failure would not necessarily originate from the tip of the breaking line, but from this suitably oriented flaw (e.g., pore, string of pores or machine flaw) above the tip of the breaking line within the loading plane. As this would apply to all orientations of the breaking line relative to the loading plane, there should hence be no difference between the tensile strength values regardless of breaking line orientation, which would match the experimental findings.

On the other hand one could argue that equation (1) represents an analytical solution for a flat tablet only without accounting for the presence of a breaking line, while the FEM model predicts the stress concentrations at various points at the surface and within the tablet without the need for such an equation. Equation (1) might simply overestimate the thickness of the loading plane by the depth of the breaking line (0.52 mm). This would, of course, only fully apply to the 0° position of the breaking line relative to the loading plane. If the values for this angle (breaking line facing down) are corrected, then for DRT and ADT tablets this results in a tensile strength of 2.37±0.16 and 3.55±0.18 MPa, respectively. These values are significantly higher ($p < 0.001$) than those obtained for all other angles between the breaking line and the loading plane. The practical results would hence confirm the FEM model predictions. This leaves the issue of the 22.5° position, where such a correction is more difficult. The angle is fairly small and for about ½ of the tablet within its centre such a correction could still be appropriate, but not for the remainder of the tablet towards its outer edges. Hence, all that could be said is that equation (1) underestimates the tensile strength of tablets with the breaking line positioned at 22.5° relative to the loading plane and therefore the brittle cracking FEM model correctly predicts a larger tensile stress.

3.3.3. Comparison using normalised stress values

Fig. 4c indicates that the x-axial tensile stresses along the z-axis towards the neutral plane are much larger than those observed for a simple bevel-edged disc, presumably due to the effect of the stress concentration above the tip of the breaking line. However, also the compressive stresses along this axis have doubled compared to a simple bevel-edged disc. This makes sense as it is normally assumed that there is a balance between tensile and compressive stresses across the XZ-plane (Benham et al., 1996).

Fig. 5c compares the normalised x-axial stresses along the y-axis. As with the fully elastic model, the stress across the lower face is reduced or similar to the stress found for a simple-bevel-edged disc. However, there is no increased normalised tensile stress at the lower face close to the bevel-edge. For breaking line positions of 45° and 22.5° again the stresses increase gradually towards the midpoint of the lower tablet face, again indicating that the discs would start to fail from the outer edges and the two initial cracks forming at each edge would propagate towards the midpoint of the discs along the loading plane until they merge and complete failure has occurred. At larger angles between breaking line and loading plane, the stresses are more likely to develop simultaneously across the loading plane, as is typically seen in simple beam-bending tests. The 0° position does again not allow a direct comparison of the stresses along the y-axis at the lower tablet face.

At the midpoint of the discs the normalised x-axial stresses along the x-axis are lower than found for a simple bevel-edged disc (Fig. 6c), most likely due to the stress concentration at the breaking line. The normalised stresses gradually increase towards the bevel-edge reaching values similar to the simple bevel-edged disc at a position close to the bevel-edge. The fluctuations seen between *2x/D=0.75-0.85* are due to overlapping tensile and compressive stresses in close proximity to the lower support rolls.

3.3.4. Comparison using absolute stress values

When the absolute values of the x-axial stresses along the y-axis at the lower surface of the discs for the three different materials studied are compared, it can be seen that there is very little difference between lactose monohydrate and the 1:1 (v/v)

powder mixture, but the stress values for acetylsalicylic acid are usually significantly lower (Fig. 8). Acetylsalicylic acid has the lowest Young's modulus and the highest critical strain energy release rate, and the combined effect of these two properties on the brittle cracking process could explain this finding. The shape of the stress profiles is fairly similar (but not identical) for the simple bevel-edged disc (Fig. 8a) and the disc with a breaking line angled 90° relative to the loading plane (Fig. 8e). In all other cases the stress concentration at the centre of the breaking line (Fig. 7b) results in a sharp drop of the absolute x-axial tensile stress values along the y-axis close to the midpoint of the discs, especially for the 22.5° (Fig. 8b) and the 45° (Fig. 8c) positions of the breaking line relative to the loading plane. The peak value for the absolute x-axial tensile stresses along the y-axis (in the figures expressed as *2y/D*) shifts from a value of 0.65 (22.5°) to 0.38 (45°) and 0.3 (67.5°) to 0.19 at the 90° position of the breaking line relative to the loading plane, i.e. from the centre towards the bevel-edge.

There is no visible difference between the three materials when the absolute values of the x-axial stresses along the z-axis for the three materials investigated are compared (results not shown). Also, the difference in the profiles when the simple bevel-edged disc is compared with discs having a breaking line positioned at 45° or larger, relative to the loading plane, is marginal. Only for breaking line positions of 0° and 22.5° larger stresses are found at the tip of the breaking lines, demonstrating their stress-concentrating effect (results not shown).

The maximum values for the x-axial tensile stresses are summarised in Table 3. The values suggest that fracture of a bevel-edged tablet with a breaking line should always start in the centre of the tablet at its lower surface, initiated by the breaking line. Due to simultaneous development of larger stresses along the y-axis the tablet will still break into two equal halves along the loading plane, unless the position of the breaking line relative to the loading plane is above 0° but less than 45°. A tablet with the breaking line positioned at, e.g., 22.5° relative to the loading plane will fail by a mixed process, whereby failure would occur mainly along the breaking line. However, due to simultaneous crack formation at the lower surface of the disc close to the bevel edge parallel to the loading plane the final breaking pattern would deviate from the breaking line about half-way from its centre.

4. Conclusions

The practical results established that, as seen in the diametral compression tests (Podczeck et al., 2014), the failure process changes with orientation of the breaking line. As expected, the failure patterns of tablets tested in diametral compression and three-point bending are entirely different and hence direct comparisons of the two studies are not appropriate unless a fracture envelope approach (Stanley, 2001) is used, which is beyond the scope of this work. In the three-point bending test it is important to ensure that the breaking line of a tablet faces either up- or downwards, as this significantly influences the tensile strength of the tablets. However, the orientation of the breaking line relative to the loading plane appears not to affect the tensile strength values significantly. An exception from to this rule is seen, when the breaking line faces upwards at the 0°-angle position relative to the loading plane. Here, the loading roll will penetrate the line cavity to some degree, preventing bending and causing load spreading, which will result in a slightly smaller, but not necessarily statistically significantly different tensile strength. If the three-point bending test were to replace the diametral compression test under routine industrial working conditions, a fairly sophisticated system would hence be required that can ensure that the breaking line is always facing downwards, preferably also always in the 0° position relative to the loading plane.

In contrast to the practical findings, the fully elastic FEM model indicates that both the position of the breaking line relative to the loading plane and as to whether the breaking line faces up- or downwards during the bending test should result in considerably different failure loads during bending experiments. The results also suggest that regardless of the breaking line position, when it is facing down crack propagation will start at the outer edges propagating towards the midpoint of the discs until failure occurs. Failure should hence always result in equal tablet halves, whereby the failure plane should coincide with the loading plane. Neither predictions fully reflected the practical behaviour of the tablets.

When using the FEM brittle cracking model the predicted crack propagation patterns were similar to those found in the experiments and in this model the stress distributions across the lower surfaces were much more homogeneous and streamlined parallel to the loading plane, as would be expected in a bending experiment. The findings suggested that with the breaking line facing down fracture

should always start in the centre of a tablet at its lower surface, initiated by the breaking line. Due to simultaneous development of larger stresses along the y-axis the tablet should still break into two equal halves along the loading plane, unless the position of the breaking line relative to the loading plane was above 0° but less than 45°. In this case the tablet would fail by a mixed process, whereby failure would occur mainly, but not fully along the breaking line. Both observations were confirmed in the practical experiments.

Significantly larger tensile strength values for tablets with the breaking line positioned 0° or 22.5° relative to the loading plane are still predicted when using the brittle cracking FEM model, but the differences between model and experimental values are greatly reduced. The remaining differences are likely due to the presence and orientation of pores within the tablets and the inadequacy of the equation available to calculate the experimental tensile strength values. This equation cannot account for the presence of a breaking line and overestimates the thickness of the loading plane by the depth of the breaking line when in the 0° or 22.5° position. If the depth of the breaking line is taken into account, the model predictions and the experimental findings are similar. The brittle cracking FEM model is hence a suitable model to investigate the tensile failure of pharmaceutical tablets. It emphasises that tablets are brittle in nature despite some of their ingredients behaving ductile during the compaction process.

Acknowledgements

The authors are grateful to Denis Cooper and Simon Carter (Engineering Systems, Nottingham, UK) for the loan of the CT6 tablet strength tester.

References

Adams, M.J., 1985. The strength of particulate solids. J. Powder Bulk Solids Technol. 9, 15-20.

Barcellos, A., 1953. Tensile strength of concrete – correlation between tensile and compressive concrete strength. RILEM Bull. 15, 109-113.

Benham, P.P., Crawford, R.J., Armstrong, C.G., 1996. Mechanics of Engineering Materials. 2nd ed., Pearson Education Limited, Harlow, pp. 135-136.

Berry, D.A., Lindgren, B.W., 1996. Statistics – Theory and Methods. 2nd ed. Duxbury Press, Belmont, pp. 577-578.

Bin Baie, S., Newton, J.M., Podczeck, F., 1996. The characterisation of the mechanical properties of pharmaceutical materials. Eur. J. Pharm. Biopharm. 43, 138-141.

Boccaccini, A., 1999. Fabrication, microstructural characterisation and mechanical properties of glass compacts containing controlled porosity of spheroidal shape. J. Porous Mater. 6, 369-379.

Boots Aspirin 300 mg Dispersible Tablets; Summary of Product Characteristics; The Boots Company Plc; Nottingham, UK, 27 April 2015.

Brown, W.F., Srawley, J.E., 1967. Plane strain crack toughness testing of high strength metallic materials. ASTM Special Technical Publ. No. 410. Am. Soc. Test. & Mater., Philadelphia, PA.

Burger, C.P., 1969. A generalized method for photoelastic studies of transient thermal stresses. Exp. Mech. 9, 529-537.

Carneiro, F.L.L., 1953. Tensile strength of concrete – a new method for determining the tensile strength of concretes. RILEM Bull. 13, 103-107.

Charlton, B., Newton, J.M., 1985. Application of gamma-ray attenuation to the determination of density distributions within compacted powders. Powder Technol. 41, 123-134.

Cole, E.T., Rees, J.E., Hersey, J.A., 1975. Relations between compaction data for some crystalline pharmaceutical materials. Pharm. Acta Helv. 50, 28-32.

Drake, K.R., Newton, J.M., Mokhtary-Saghafi, S., Davies, P.N., 2007. Tensile stresses generated in pharmaceutical tablets by opposing compressive line loads. Eur. J. Pharm. Sci. 30, 273-279.

Duberg, M., Nyström, C., 1982. Studies on direct compression of tablets. VI. Evaluation of methods for the estimation of particle fragmentation during compaction. Acta Pharm. Suec. 19, 421-436.

Duncan-Hewitt, W.C., Weatherly, G.C., 1989. Evaluating the hardness, Young's modulus and fracture toughness of some pharmaceutical crystals using microindentation techniques. J. Mater. Sci. Lett. 8, 1350-1352.

Dunn, M.L., Suwito, W., Cunningham, S., 1997. Fracture initiation at sharp notches: correlation using critical stress intensities. Int. J. Solid Struct. 34, 3873-3883.

Evans, A.G., Tappin, G., 1972. Effects of microstructure on the stress to propagate inherent flaws. Proc. Br. Ceram. Soc. 20, 275-297.

Fell, J.T., Newton, J.M., 1968. The tensile strength of lactose tablets. J. Pharm. Pharmacol. 20, 657-658.

Fell, J.T., Newton, J.M., 1970. Determination of tablet strength by the diametral compression test. J. Pharm. Sci. 59, 688-691.

Fleck, N.A., Smith, R.A., 1981. Effect of density on tensile strength, fracture toughness, and fatigue crack propagation behaviour of sintered steel. Powder Metall. 3, 121-125.

Griffith, A.A., 1920. The phenomena of rupture and flow in solids. Trans. Roy. Soc. Series A 221, 163-198.

Hertzberg, R.W., 1996. Deformation and Fracture Mechanics of Engineering Materials. 4th ed., Wiley, New York, p. 43; pp. 261-313.

Humbert-Droz, P., Gurny, R., Mordier, D., Doelker, E., 1983. Densification behaviour of drugs presenting availability problems. Int. J. Pharm. Tech. & Prod. Mfr. 4, 29-35.

Irwin, G.R., 1957. Analysis of stresses and strains near the end of a crack traversing a plate. J. Appl. Mech. 24, 361-364.

Jetzer, W., Düggelin, M., Guggenheim, R., Leuenberger, H., 1984. Raster-elektronenmikroskopische Untersuchungen von Wechselwirkungen beim Verpressen von binären Pulvermischungen. Acta Pharm. Technol. 30, 126-131.

Mashadi, A.B., Newton, J.M., 1987. Assessment of the mechanical properties of compacted sorbitol instant. J. Pharm. Pharmacol. 39, 67P.

Mashadi, A.B., Newton, J.M., 1988. Determination of the critical stress intensity factor (K_{IC}) of compacted pharmaceutical powders by the double-torsion method. J. Pharm. Pharmacol. 40, 597-600.

Mazel, V., Diarra, H., Busignies, V., Tchoreloff, P., 2014. Comparison of different failure tests for pharmaceutical tablets: Applicability of the Drucker-Prager failure criterion. Int. J. Pharm. 470, 63-69.

Mielck, J.B., Stark, G., 1995. Tabletting of powder mixtures: parameters of evolved pressure-time profiles indicate percolation thresholds during tabletting. Eur. J. Pharm. Biopharm. 41, 206-214.

Mullier, M.A., Seville, J.P.K., Adams, M.J., 1991. The effect of agglomerate strength on attrition during processing. Powder Technol. 65, 321-333.

Newton, J.M., Stanley, P., Tan, C.S., 1977. Model study of stresses in grooved tablets under diametral compression. J. Pharm. Pharmacol. 29, 40P.

Nicklasson, H., Podczeck, F., 2007. Evaluation of the role of pores during strength testing in compacts made from different particle size fractions of sucrose. Chem. Pharm. Bull. 55, 29-33.

Pitt, K.G., Heasley, M.G., 2013. Determination of the tensile strength of elongated tablets. Powder Technol. 238, 169-175.

Pitt, K.G., Newton, J.M., Stanley, P., 1989. Stress distributions in doubly convex cylindrical discs under diametral loading. J. Phys. D: Appl. Phys. 22, 1114-1127.

Podczeck, F., 2001a. Investigations into the fracture mechanics of acetylsalicylic acid and lactose monohydrate. J. Mater. Sci. 36, 4687-4693.

Podczeck, F., 2001b. The determination of fracture mechanics properties of pharmaceutical materials in mode III loading using an anti-clastic plate bending method. Int. J. Pharm. 227, 39-46.

Podczeck, F., 2002. The determination of the critical stress intensity factor in mode II loading and the shear fracture strength of pharmaceutical powder specimens. J. Mater. Sci. 37, 3593-3598.

Podczeck, F., 2011. Theoretical and experimental investigations into the delamination tendencies of bilayer tablets. Int. J. Pharm. 408, 102-112.

Podczeck, F., 2012. Methods for the practical determination of the mechanical strength of tablets – From empiricism to science. Int. J. Pharm. 436, 214-232.

Podczeck, F., Drake, K.R., Newton, J.M., 2013. Investigations into the tensile failure of doubly-convex cylindrical tablets under diametral loading using finite element methodology. Int. J. Pharm. 454, 412-424.

Podczeck, F., Newton, J.M., Fromme, P., 2014. Theoretical investigations into the influence of the position of a breaking line on the tensile failure of flat, round, bevel-edged tablets using finite element methodology (FEM) and its practical relevance for industrial tablet strength testing. Int. J. Pharm. 477, 306-316.

Rice, J.R., 1978. Thermodynamics of the quasi-static growth of Griffith cracks. J. Mech. Phys. Solids 26, 61-78.

Rice, R.W., 1984. Pores as fracture origins in ceramics. J. Mater. Sci. 19, 895-914.

Rice, R.W., 1989. Relation of tensile strength–porosity effects in ceramics to porosity dependence of Young's modulus and fracture energy, porosity character and grain size. Mater. Sci. Eng. A112, 215-224.

Rice, R.W., 1994. Porosity effects on machining direction – strength anisotropy and failure mechanisms. J. Am. Ceram. Soc. 77, 2232-2236.

Roberts, R.J., Rowe, R.C., 1987. Brittle/ductile behaviour in pharmaceutical materials used in tabletting. Int. J. Pharm. 36, 205-209.

Roberts, R.J., Rowe, R.C., York, P., 1993. The measurement of the critical stress intensity factor (K_{IC}) of Pharmaceutical powders using three point single edge notched beam (SENB) testing. Int. J. Pharm. 91, 173-182.

Scheffé, H., 1959. The Analysis of Variance. Wiley, New York; (reprinted 1999, ISBN 0-471-34505-9).

Stanley, P., 2001. Mechanical strength testing of compacted powders. Int. J. Pharm. 227, 27-38.

Stanley, P., Newton, J.M., 1978. Variability in the strength of powder compacts. J. Powder Bulk Solids Tech. 1, 13-19.

Szibor, H., Hennicke, H.W., 1982. Zum Zusammenhang von Gefügedaten und mechanischen Eigenschaften von Porzellanwerkstoffen, Teil II. Ber. Dt. Keram. Ges. 59, 170-175.

Timoshenko, S.P., Goodier, J.N., 1987. Theory of Elasticity. 3rd ed. McGraw-Hill, New York.

Train, D., 1957. Transmission of forces through a powder mass during the process of pelleting. Trans. Instn. Chem. Engrs. 35, 258-266.

USP38/NF33 (United States Pharmacopoeia/National Formulary), 2014. Tablet Breaking Force (Method 1217). The United States Pharmacopoeial Convention, Rockville, MD.

Van Santen, E., Barends, D.M., Frijlink, H.W., 2002. Breaking of scored tablets: a review. Eur. J. Pharm. Biopharm. 53, 139-145.

Wu, Y.S., Frijlink, H.W., van Vliet, L.J., Stokroos, I., van der Voort Maarschalk, K., 2005. Location-dependent analysis of porosity and pore direction in tablets. Pharm. Res. 22, 1399-1405.

Young, L.L., 1995. Tableting Specification Manual. American Pharmaceutical Association, Washington, DC, p. 46.

Legends to Figures

Figure 1

Tablet modelling. (a) Basic terminology of flat, round, bevel-edged tablets (Young, 1995) with a breaking line. *W* = tablet thickness; *B* = band thickness; *C* = cup depth; *D* = tablet diameter; α = bevel angle (30°). (b) FEM model of a three-point tablet bending process. φ = angle between the breaking line and the loading plane. Boundary conditions: upper roll $u_x=u_y=0$; $R_x=R_y=R_z=0$; lower rolls: $u_x=u_y=u_z=0$; $R_x=R_y=R_z=0$.

Figure 2

Breaking patterns of tablets with a breaking line, subjected to three-point bending, with the breaking line facing down at an angle φ relative to the loading plane. (a) DRT tablet at φ = 22.5°; (b) ADT tablet at φ = 22.5°; (c) ADT tablet at φ = 90°; (d) ADT tablet at φ = 45°.

Figure 3

The x-axial stress distribution in elastic discs with breaking line during three-point bending. (a) XZ-Plane (section through the centre of the disc; areas of compressive stresses are shaded grey); (b) XY-Plane at the lower surface.

Figure 4

Normalised x-axial stresses along the z-axis (depth; coordinates $x=y=0$), obtained on (a) elastic discs with the breaking line facing down; (b) elastic discs with the breaking line facing up; (c) brittle lactose monohydrate discs with the breaking line facing down. The abscissa shows the position along the z-axis starting at the lower side (-1.0) and progressing towards the upper side of the disc (+1.0).

Figure 5

Normalised x-axial stresses along the y-axis (coordinates $x=0;\ z=-0.5$), obtained on (a) elastic discs with the breaking line facing down; (b) elastic discs with the breaking

line facing up; (c) brittle lactose monohydrate discs with the breaking line facing down. The abscissa shows the position along the y-axis starting at the midpoint (0.0) and progressing towards the edge of the disc (+1.0).

Figure 6

Normalised x-axial stresses along the x-axis (coordinates y=*0; z= -0.5*), obtained on (a) elastic discs with the breaking line facing down; (b) elastic discs with the breaking line facing up; (c) brittle lactose monohydrate discs with the breaking line facing down. The abscissa shows the position along the x-axis starting at the midpoint (0.0) and progressing towards the edge of the disc (+1.0).

Figure 7

The x-axial stress distribution and crack propagation in brittle lactose monohydrate discs with breaking line during three-point bending. (a) XZ-Plane (section through the centre of the disc; areas of compressive stress are shaded grey); (b) XY-Plane at the lower surface.

Figure 8

Absolute values of x-axial stresses [MPa] along the y-axis (coordinates *x=0; z=-0.5*), for (a) bevel-edged discs; and discs with the breaking line facing down positioned at an angle φ of (b) 22.5°; (c) 45°; (d) 67.5°; (e) 90°. The abscissa shows the position along the y-axis starting at the midpoint (0.0) and progressing towards the edge of the disc (+1.0).

Legends to Tables

Table 1

Material properties used in FEM “brittle cracking” simulations. LM = lactose monohydrate; ASS = acetylsalicylic acid.

Table 2

Tablet properties obtained on two commercially produced batches of tablets with a breaking line. φ = angle between the breaking line and the upper bending roll; W = thickness; D = diameter; w = weight; p = porosity; σ_t = tensile strength; DRT = Diarrhoea Relief Tablets; ADT = Aspirin Dispersible Tablets; DN = breaking line facing down; UP = breaking line facing up. Results are arithmetic mean ± standard deviation of ten tablets.

Table 3

Comparison of the maximum x-axial tensile stresses [MPa] along the y- and z-axis obtained using different FEM models and different fracture mechanics properties (see Table 1); φ = angle between the breaking line and the upper bending roll; values in brackets are taken from the tip of the crack due to the crack position.

Table 1

Material properties used in FEM “brittle cracking” simulations. LM = lactose monohydrate; ASS = acetylsalicylic acid.

Material Property	LM[a)]	ASS[a)]	Powder mixture[b)] LM:ASS 1:1 (v/v)
Density [kg m^{-3}]	1540	1400	1470
Max. failure stress [MPa]	33.04	13.00	13.44
Young’s modulus [GPa]	2.99	1.51	1.99
Poisson’s ratio	0.3	0.3	0.3
Critical stress intensity factor [kPa $m^{0.5}$]	493	355	395
	73.97	75.95	71.35
Critical strain energy release rate [N m^{-1}]			

[a)]Podczeck, 2001a

[b)]Podczeck, 2011

Table 2

Tablet properties obtained on two commercially produced batches of tablets with a breaking line.

φ = angle between the breaking line and the upper bending roll; W = thickness; D = diameter; w = weight; p = porosity; σ_t = tensile strength; DRT = Diarrhoea Relief Tablets; ADT = Aspirin Dispersible Tablets; DN = breaking line facing down; UP = breaking line facing up. Results are arithmetic mean ± standard deviation of ten tablets.

Batch	φ	W [mm]	D [mm]	w [mg]	p	σ_t [MPa]
DRT; DN	0°	3.658 ± 0.037	12.815 ± 0.005	800 ± 9	0.211 ± 0.005	1.75 ± 0.11
	22.5°	3.684 ± 0.028	12.827 ± 0.006	804 ± 7	0.214 ± 0.007	1.80 ± 0.10
	45°	3.670 ± 0.039	12.815 ± 0.005	801 ± 12	0.213 ± 0.007	1.84 ± 0.10
	67.5°	3.670 ± 0.039	12.836 ± 0.018	799 ± 11	0.217 ± 0.005	1.82 ± 0.10
	90°	3.668 ± 0.026	12.828 ± 0.006	798 ± 11	0.217 ± 0.006	1.87 ± 0.14
DRT; UP	0°	3.676 ± 0.025	12.828 ± 0.006	807 ± 7	0.210 ± 0.004	1.80 ± 0.10
	22.5°	3.672 ± 0.024	12.829 ± 0.006	808 ± 8	0.208 ± 0.007	1.92 ± 0.12
	45°	3.675 ± 0.031	12.821 ± 0.007	804 ± 6	0.211 ± 0.002	2.01 ± 0.18

	67.5°	3.664 ± 0.031	12.819 ± 0.006	803 ± 12	0.210 ± 0.006	1.94 ± 0.18
	90°	3.682 ± 0.028	12.823 ± 0.007	810 ± 10	0.207 ± 0.005	1.98 ± 0.13
ADT; DN	0°	3.656 ± 0.018	12.992 ± 0.023	606 ± 5	0.150 ± 0.002	2.61 ± 0.14
	22.5°	3.646 ± 0.037	12.996 ± 0.027	605 ± 8	0.149 ± 0.005	2.62 ± 0.19
	45°	3.654 ± 0.041	12.983 ± 0.017	604 ± 8	0.151 ± 0.004	2.77 ± 0.18
	67.5°	3.623 ± 0.018	12.996 ± 0.024	598 ± 14	0.153 ± 0.003	2.70 ± 0.17
	90°	3.628 ± 0.034	12.985 ± 0.034	600 ± 8	0.150 ± 0.005	2.85 ± 0.25
ADT; UP	0°	3.609 ± 0.054	12.989 ± 0.026	596 ± 11	0.152 ± 0.004	2.68 ± 0.15
	22.5°	3.612 ± 0.028	12.981 ± 0.014	595 ± 6	0.152 ± 0.004	2.72 ± 0.25
	45°	3.627 ± 0.038	12.984 ± 0.022	598 ± 6	0.153 ± 0.008	2.65 ± 0.15
	67.5°	3.637 ± 0.035	12.987 ± 0.014	602 ± 7	0.150 ± 0.004	2.88 ± 0.29
	90°	3.635 ± 0.043	12.989 ± 0.024	602 ± 10	0.150 ± 0.009	2.93 ± 0.31

Table 3

Comparison of the maximum x-axial tensile stresses [MPa] along the y- and z-axis obtained using different FEM models and different fracture mechanics properties (see Table 1); φ = angle between the breaking line and the upper bending roll; values in brackets are taken from the tip of the crack due to the crack position.

	y-axis (coordinates *x=0; z=-0.5*)	z-axis (coordinates *x=y=0*)
Fully Elastic Model		
Bevel edged tablet	1.807	1.807
φ=0°	(8.271)	7.298
φ=22.5°	1.177	4.842
φ=45°	1.551	2.240
φ=67.5°	1.741	2.308
φ=90°	1.840	1.308
Brittle Cracking Model		
Lactose monohydrate		
Bevel edged tablet	1.143	1.141
φ=0°	(4.528)	3.644
φ=22.5°	0.831	2.820
φ=45°	1.031	1.427
φ=67.5°	1.118	1.415

φ=90°	1.129	1.029
Acetylsalicylic acid		
Bevel edged tablet	1.076	1.075
φ=0°	(4.119)	3.318
φ=22.5°	0.756	2.569
φ=45°	0.909	1.327
φ=67.5°	0.988	1.250
φ=90°	1.023	0.997
Powder mixture		
Bevel edged tablet	1.123	1.120
φ=0°	(4.401)	3.543
φ=22.5°	0.802	2.742
φ=45°	1.005	1.397
φ=67.5°	1.095	1.394
φ=90°	1.107	1.015

Figure 1

Tablet modelling.

(a) Basic terminology of flat, round, bevel-edged tablets (Young, 1995) with a breaking line. *W* = tablet thickness; *B* = band thickness; *C* = cup depth; *D* = tablet diameter; α = bevel angle (30°).

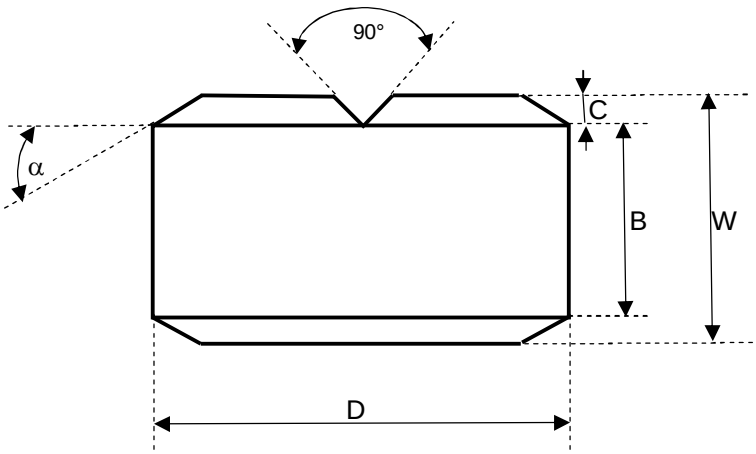

(b) FEM model of a three-point tablet bending process. φ = angle between the breaking line and the loading plane. Boundary conditions: upper roll $u_x=u_y=0$; $R_x=R_y=R_z=0$; lower rolls: $u_x=u_y=u_z=0$; $R_x=R_y=R_z=0$.

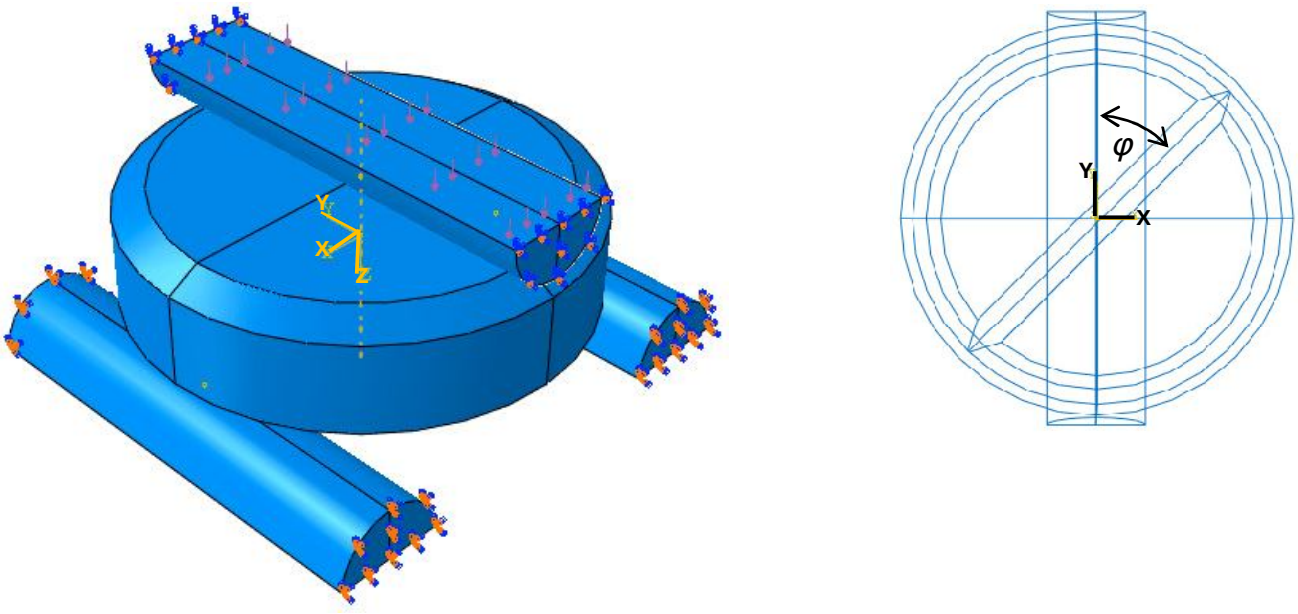

Figure 2

Breaking patterns of tablets with a breaking line, subjected to three-point bending, with the breaking line facing down at an angle φ relative to the loading plane.

(a) DRT tablet at $\varphi = 22.5°$; (b) ADT tablet at $\varphi = 22.5°$; (c) ADT tablet at $\varphi = 90°$; (d) ADT tablet at $\varphi = 45°$.

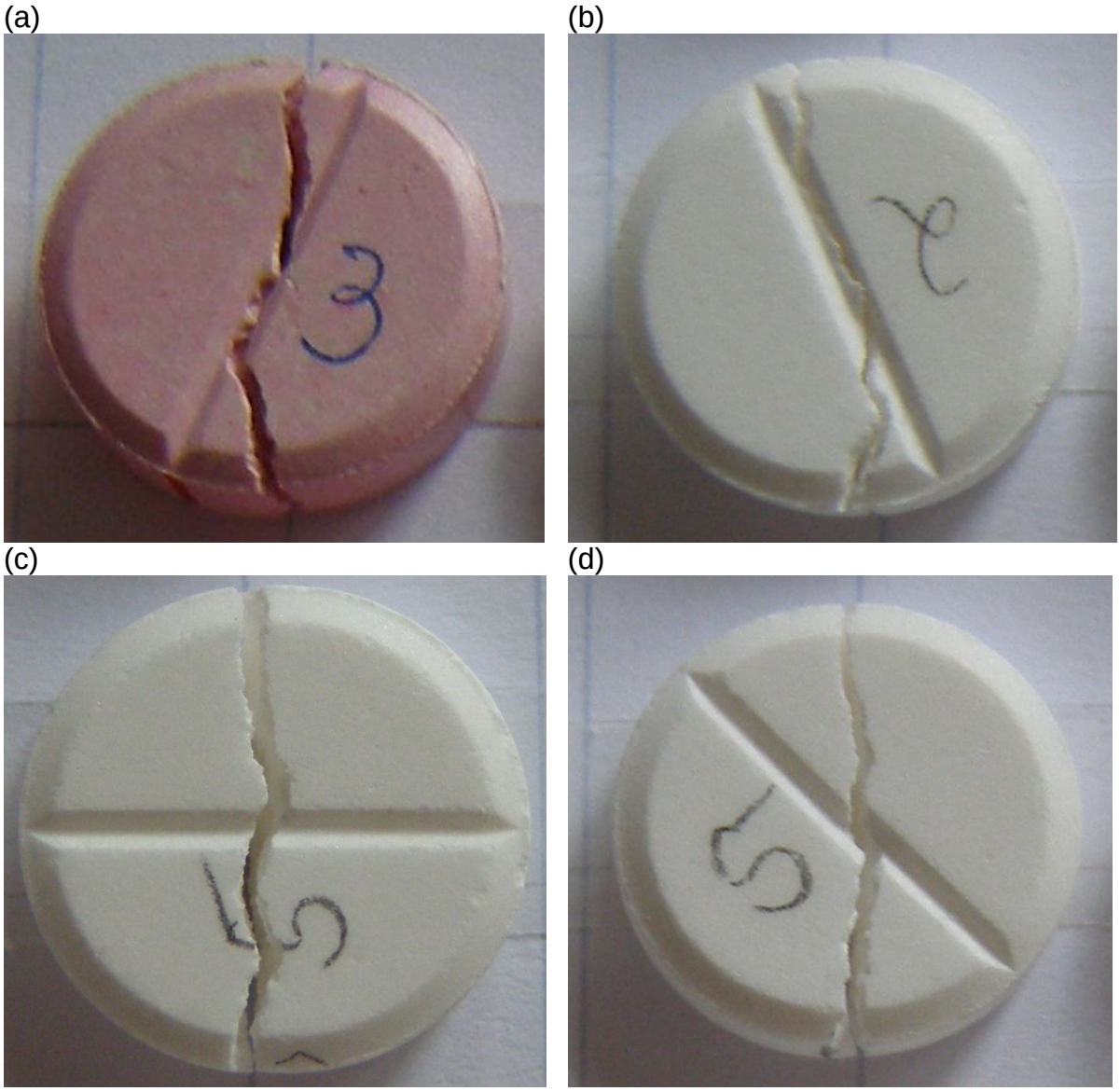

Figure 3a

The x-axial stress distribution in elastic discs with breaking line during three-point bending – (a) XZ-Plane (section through the centre of the disc; areas of compressive stresses are shaded grey).

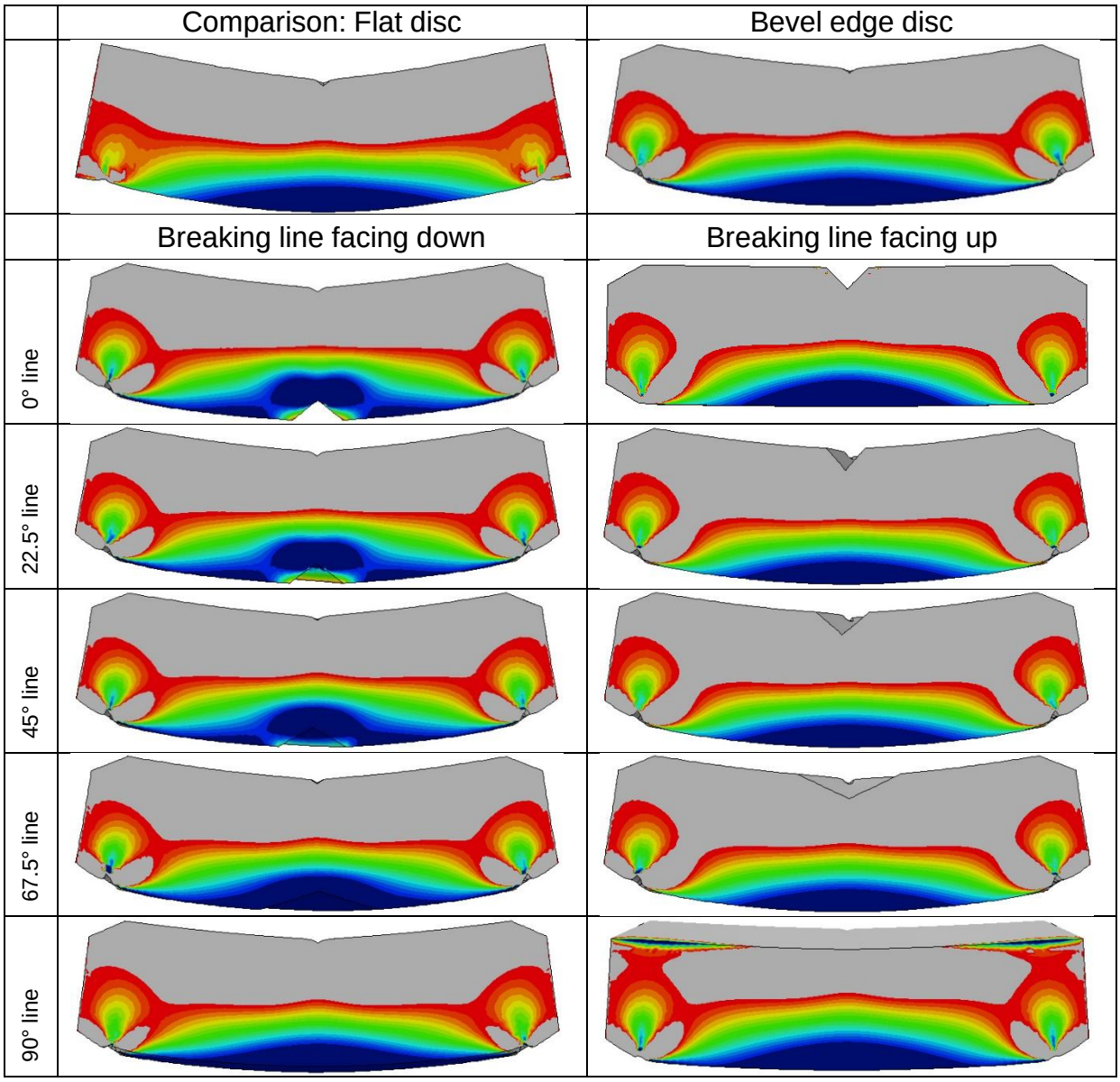

Figure 3b

The x-axial stress distribution in elastic discs with breaking line during three-point bending – (b) XY-Plane at the lower surface.

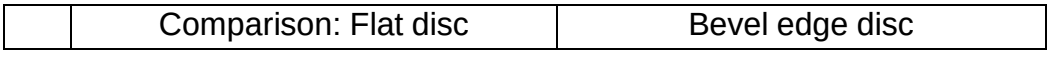

	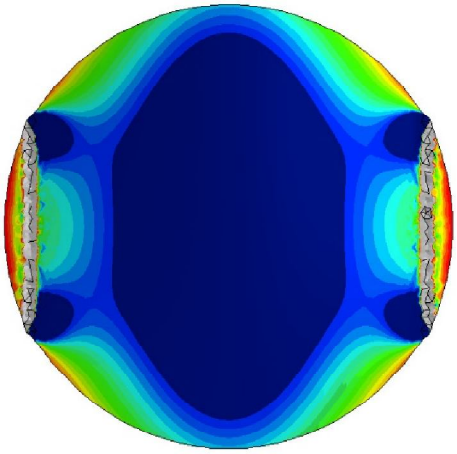	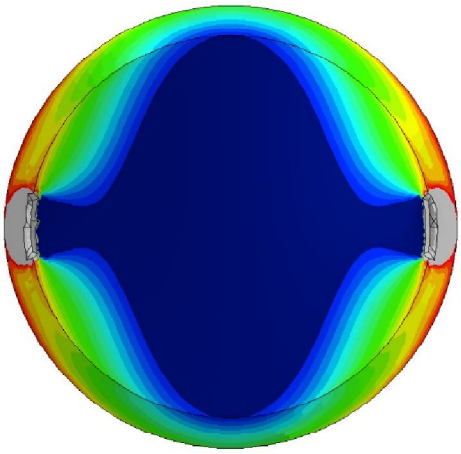
	Lower surface, breaking line facing down	Lower surface, breaking line facing up
0° breaking line	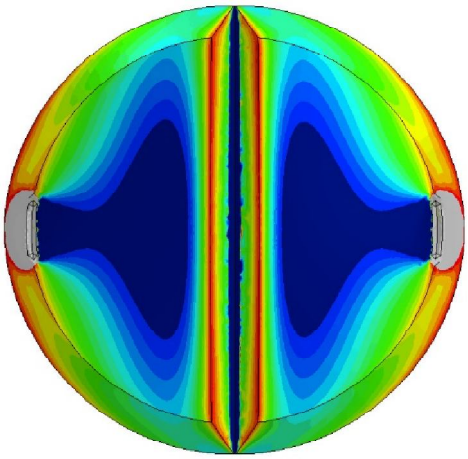	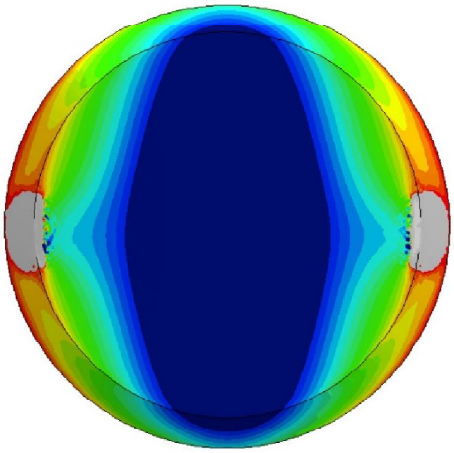
22.5° breaking line	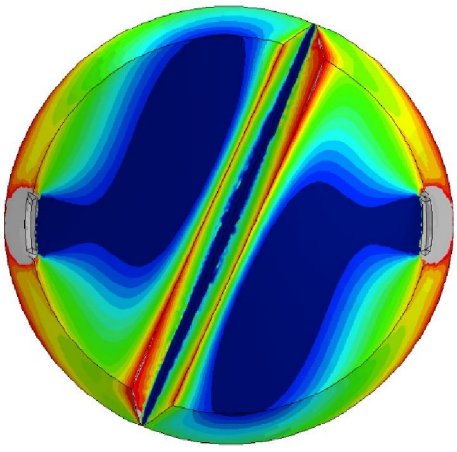	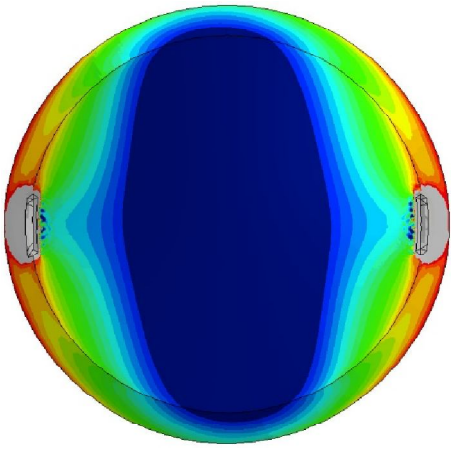

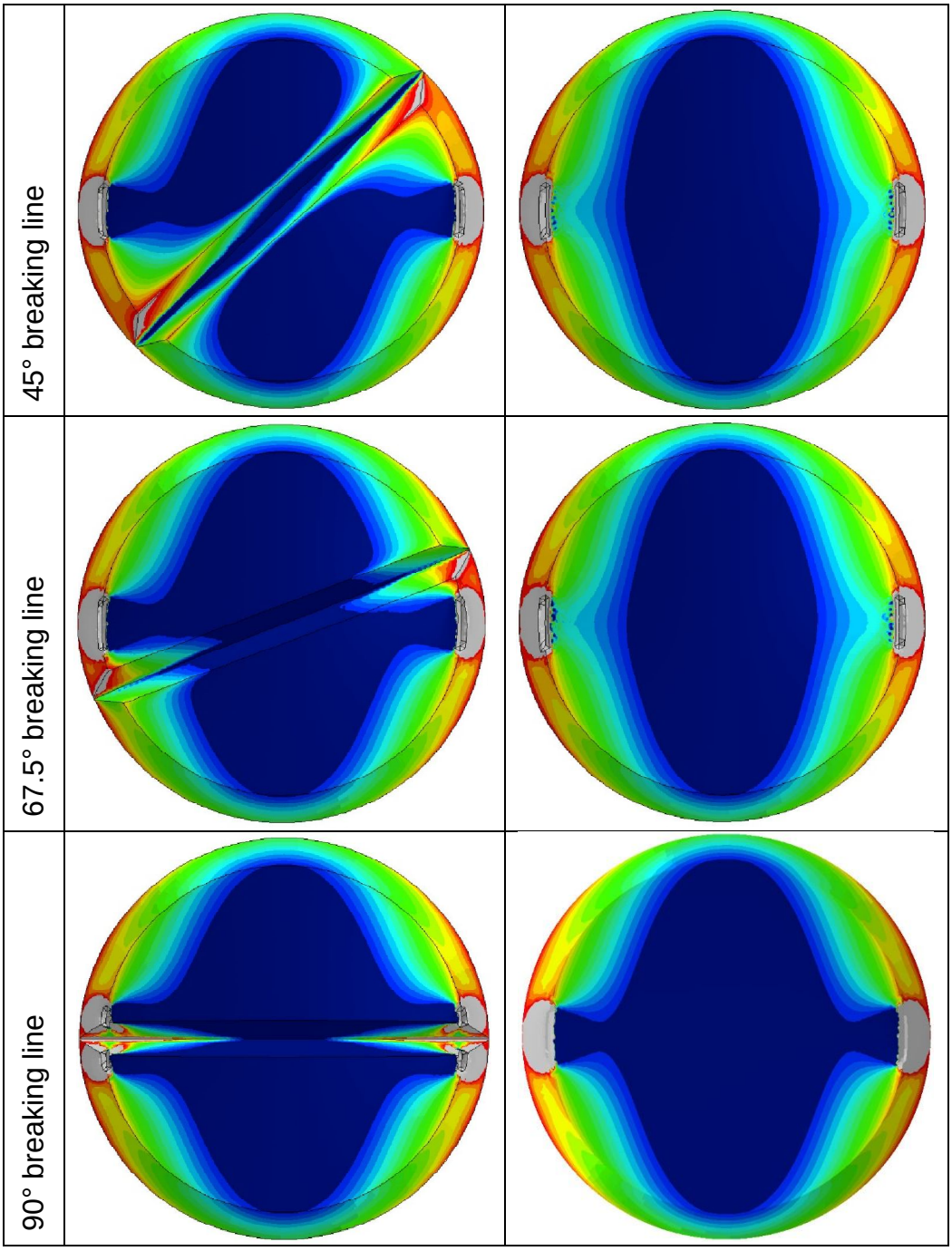

Figure 3b (continued)

Figure 4

Normalised x-axial stresses along the z-axis (depth; coordinates *x=y=0*), obtained on (a) elastic discs with the breaking line facing down; (b) elastic discs with the breaking line facing up; (c) brittle lactose monohydrate discs with the breaking line facing down. The abscissa shows the position along the z-axis starting at the lower side (-1.0) and progressing towards the upper side of the disc (+1.0).

(a)

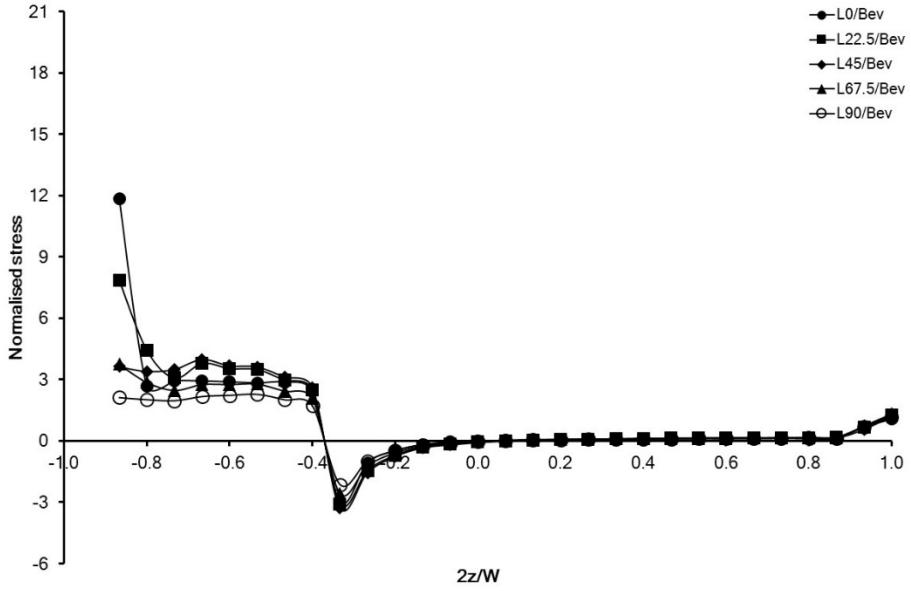

(b)

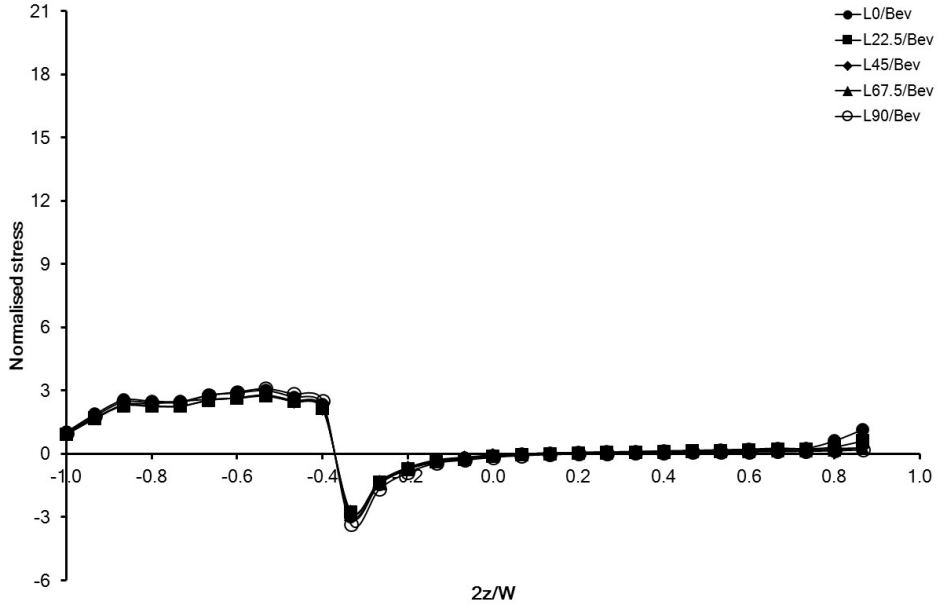

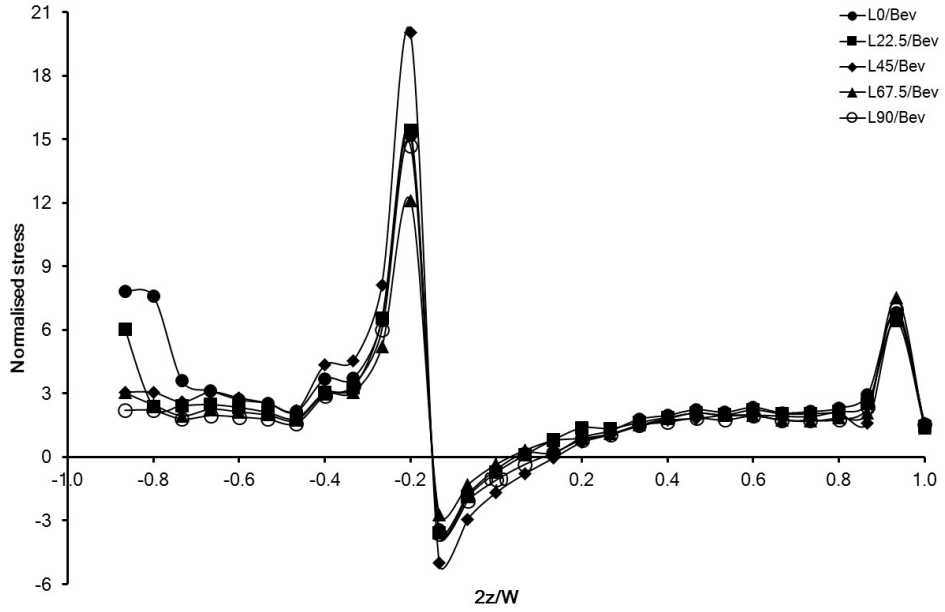

(c)

Figure 5

Normalised x-axial stresses along the y-axis (coordinates *x=0; z= -0.5*), obtained on (a) elastic discs with the breaking line facing down; (b) elastic discs with the breaking line facing up; (c) brittle lactose monohydrate discs with the breaking line facing down. The abscissa shows the position along the y-axis starting at the midpoint (0.0) and progressing towards the edge of the disc (+1.0).

(a)

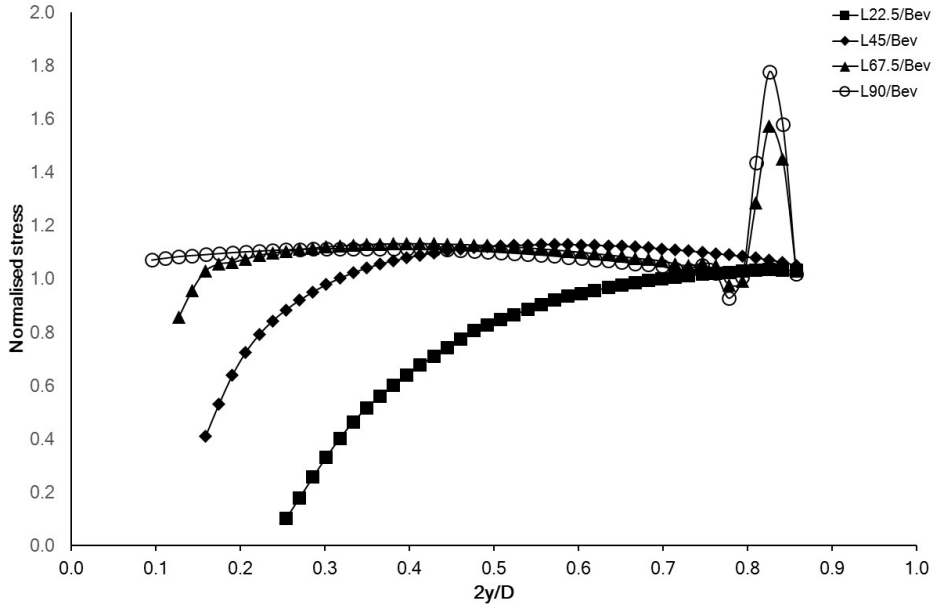

(b)

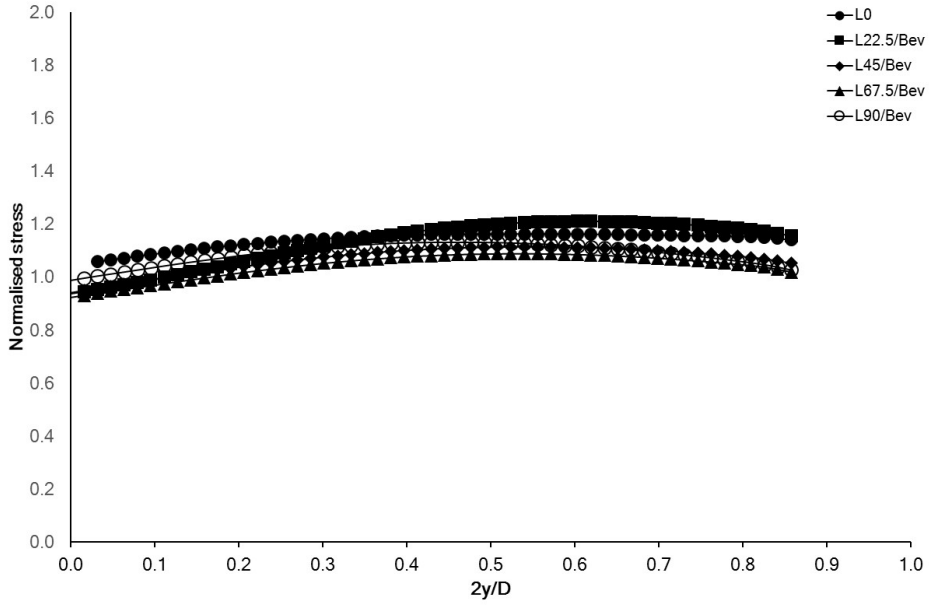

(c)

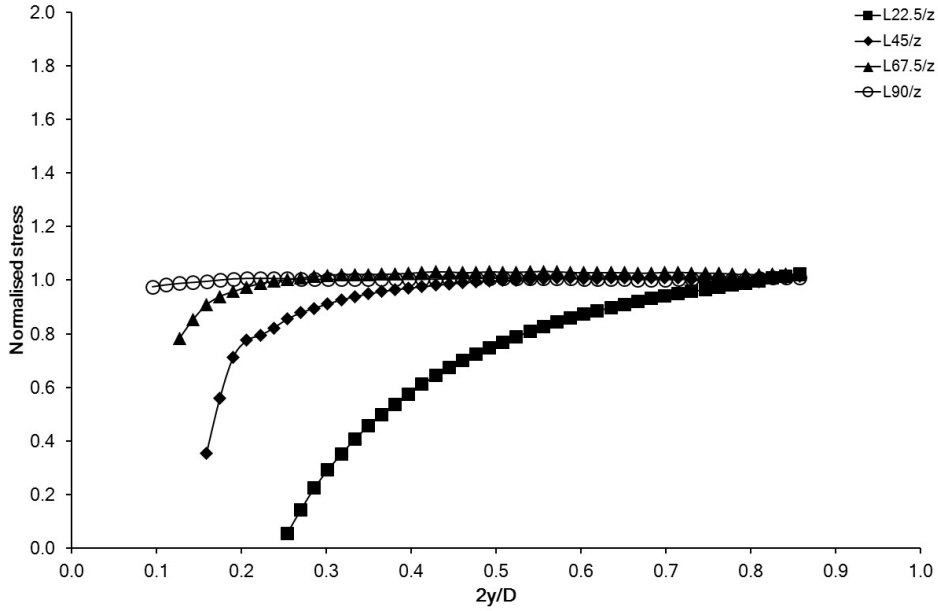

Figure 6

Normalised x-axial stresses along the x-axis (coordinates y=*0; z= -0.5*), obtained on (a) elastic discs with the breaking line facing down; (b) elastic discs with the breaking line facing up; (c) brittle lactose monohydrate discs with the breaking line facing down. The abscissa shows the position along the x-axis starting at the midpoint (0.0) and progressing towards the edge of the disc (+1.0).

(a)

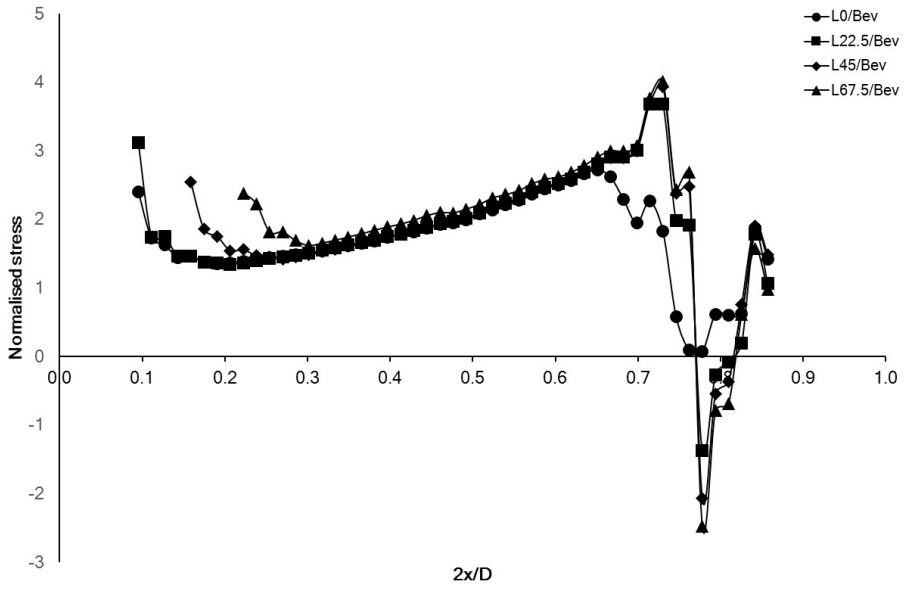

(b)

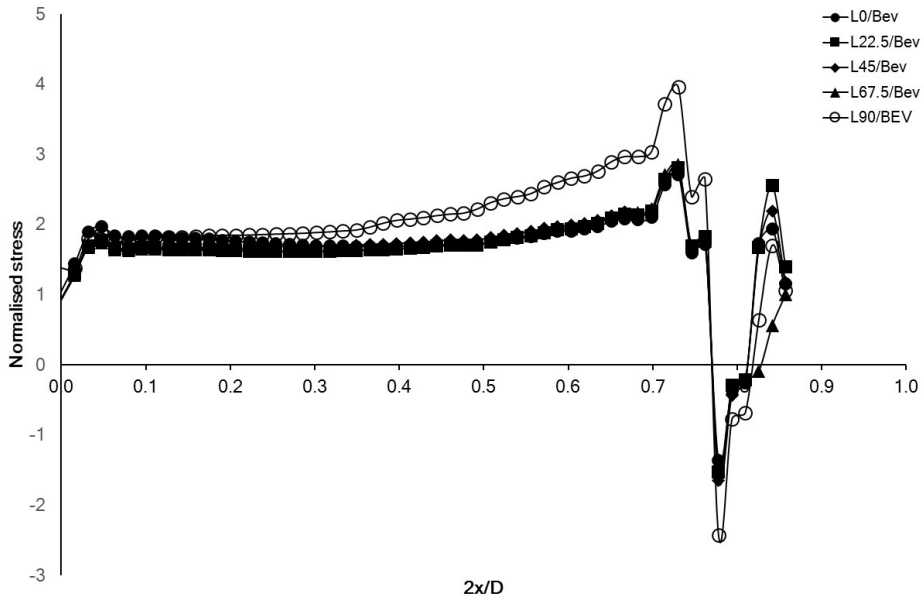

(c)

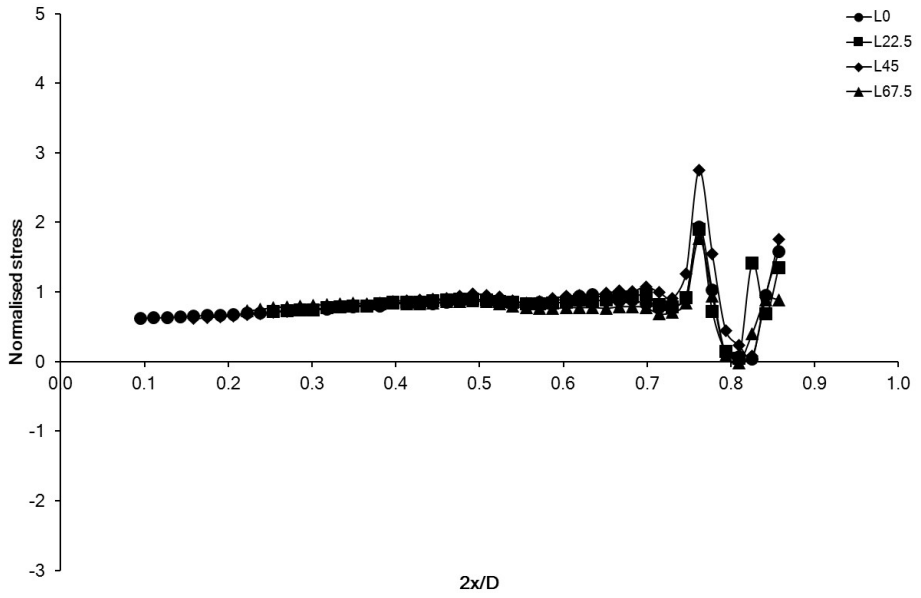

Figure 7a

The x-axial stress distribution and crack propagation (→) in brittle lactose monohydrate discs with breaking line during three-point bending – (a) XZ-Plane (section through the centre of the disc; areas of compressive stresses are shaded grey).

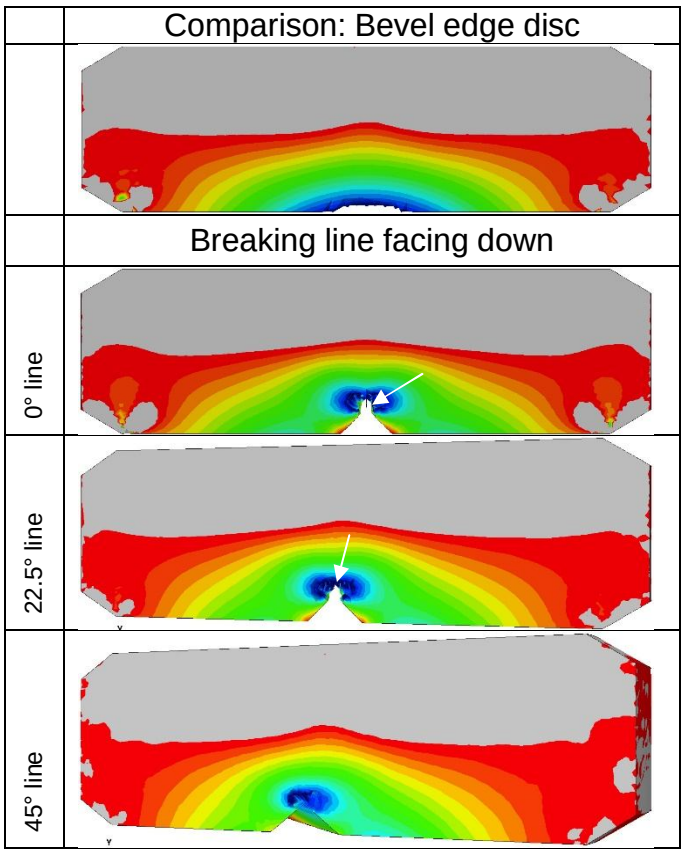

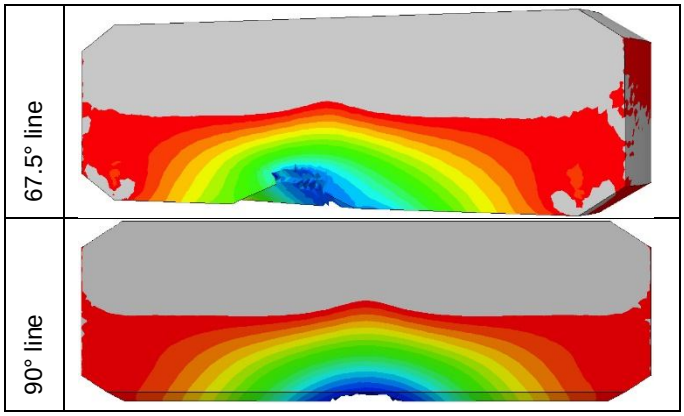

Figure 7b

The x-axial stress distribution and crack propagation (→) in brittle lactose monohydrate discs with breaking line during three-point bending. (b) XY-Plane at the lower surface.

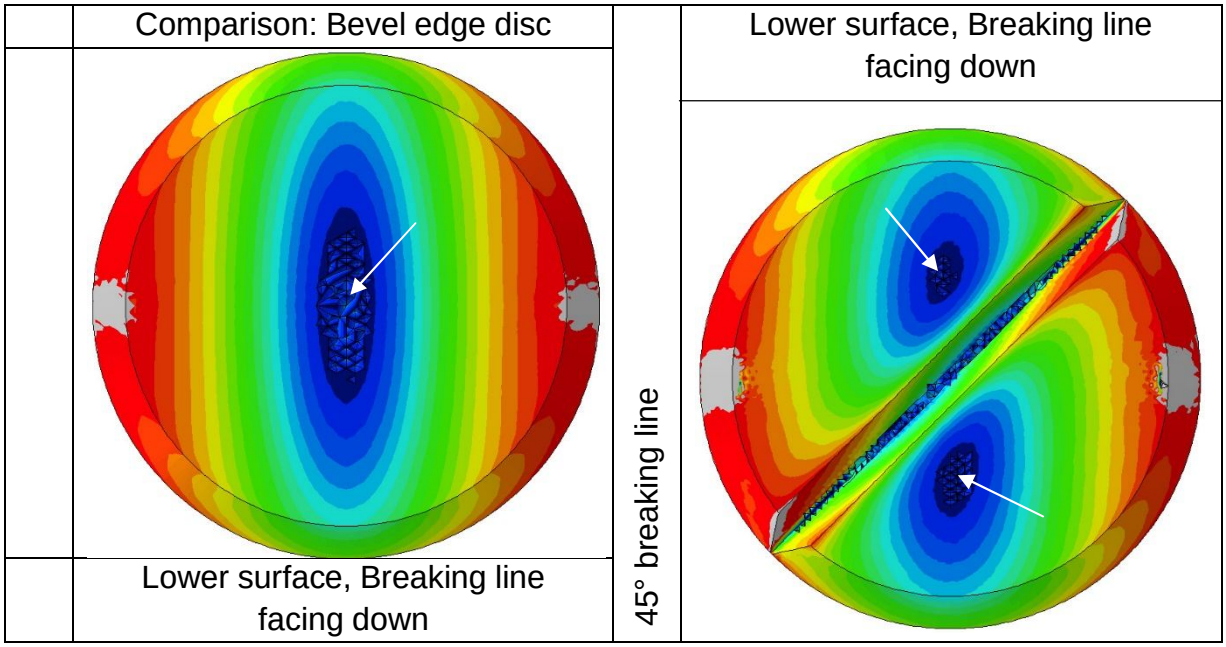

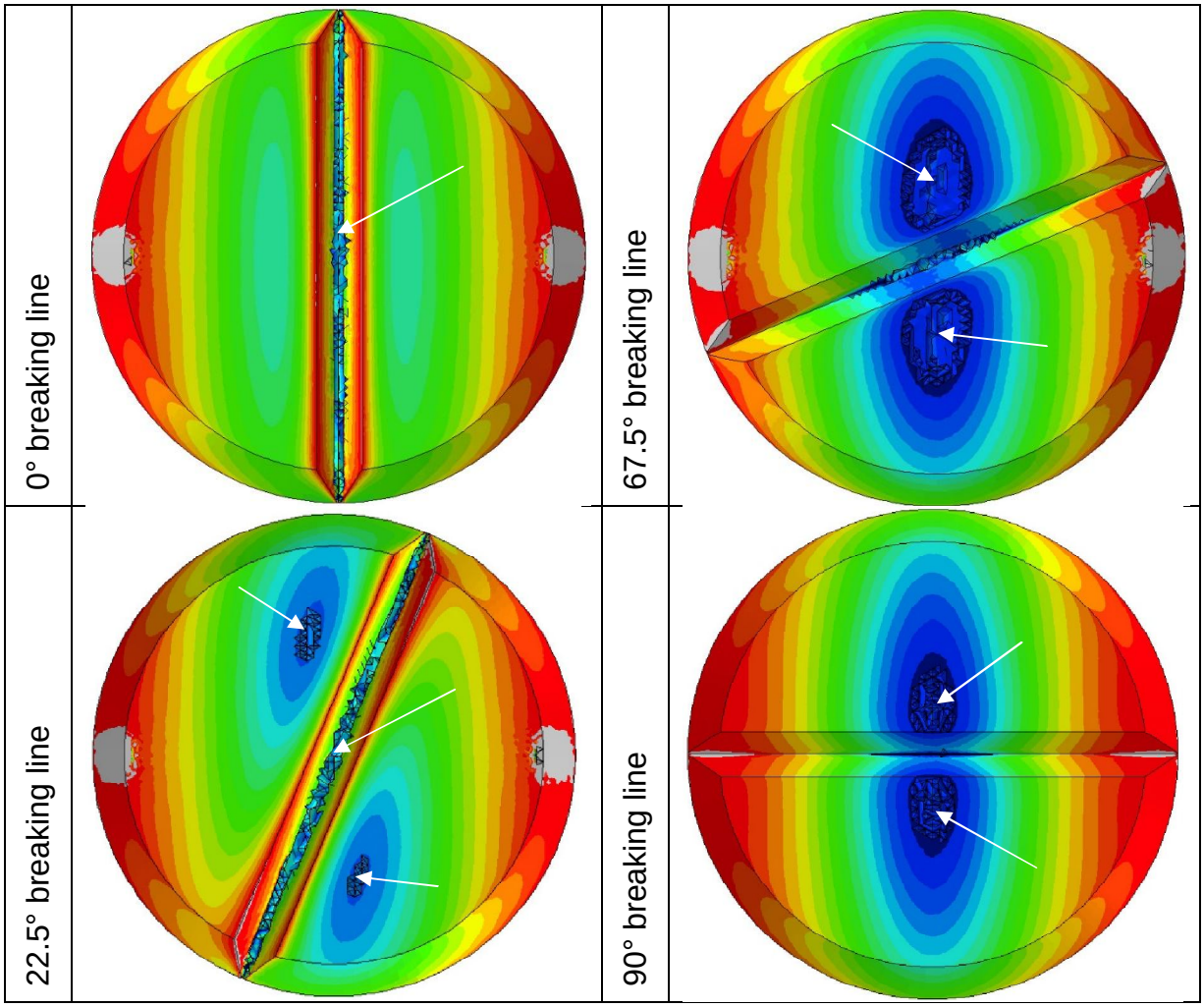

Figure 8

Absolute values of x-axial stresses [MPa] along the y-axis (coordinates *x=0; z=-0.5*), for (a) bevel-edged discs; and discs with the breaking line facing down positioned at an angle φ of (b) 22.5°; (c) 45°; (d) 67.5°; (e) 90°. The abscissa shows the position along the y-axis starting at the midpoint (0.0) and progressing towards the edge of the disc (+1.0).

(a)

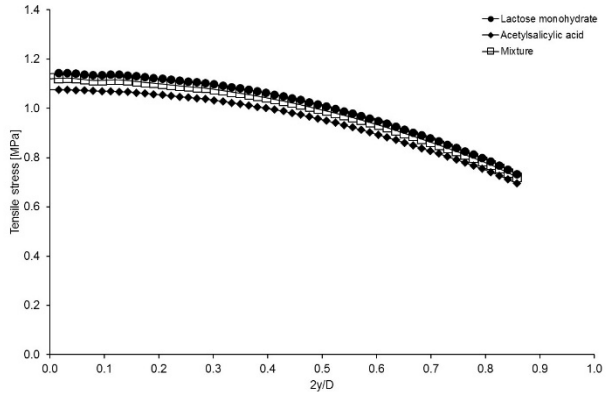

(b)

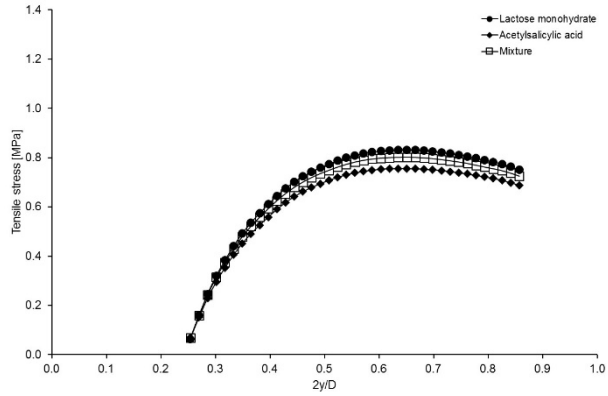

(c)

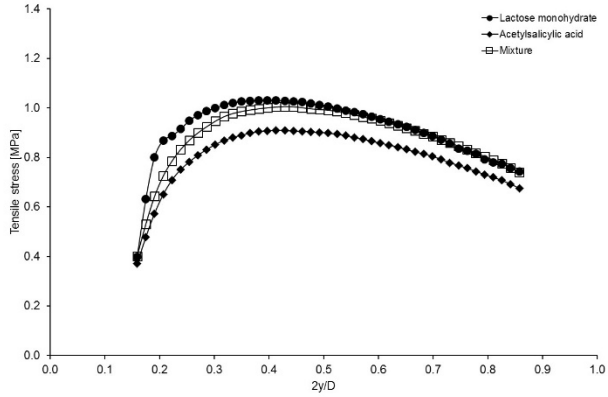

(d)

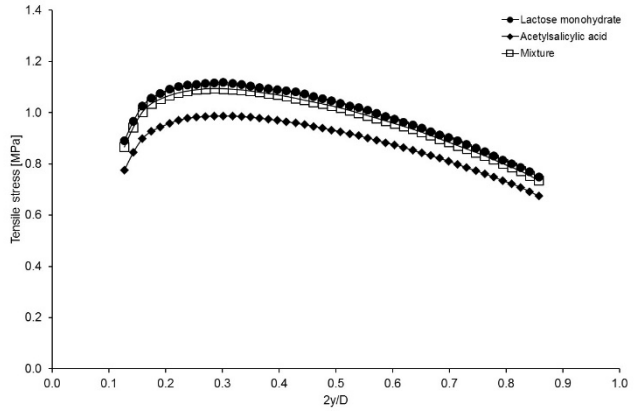

(e)